The Plant Cell, Vol. 24: 482–506, February 2012, www.plantcell.org © 2012 American Society of Plant Biologists. All rights reserved.

JUNGBRUNNEN1, a Reactive Oxygen Species–Responsive NAC Transcription Factor, Regulates Longevity in *Arabidopsis* [W] [OA]

Anhui Wu,[a,b,1] Annapurna Devi Allu,[a,b,1] Prashanth Garapati,[a,b] Hamad Siddiqui,[a] Hakan Dortay,[a] Maria-Inés Zanor,[b] Maria Amparo Asensi-Fabado,[c] Sergi Munné-Bosch,[c] Carla Antonio,[b] Takayuki Tohge,[b] Alisdair R. Fernie,[b] Kerstin Kaufmann,[d] Gang-Ping Xue,[e] Bernd Mueller-Roeber,[a,b,2] and Salma Balazadeh[a,b]

[a] University of Potsdam, Institute of Biochemistry and Biology, 14476 Potsdam-Golm, Germany
[b] Max-Planck Institute of Molecular Plant Physiology, 14476 Potsdam-Golm, Germany
[c] Departament de Biologia Vegetal, Universitat de Barcelona, Facultat de Biologia, 08028 Barcelona, Spain
[d] Laboratory of Molecular Biology, Wageningen University, 6708 PB Wageningen, The Netherlands
[e] CSIRO Plant Industry, St. Lucia QLD 4067, Australia

The transition from juvenility through maturation to senescence is a complex process that involves the regulation of longevity. Here, we identify *JUNGBRUNNEN1* (*JUB1*), a hydrogen peroxide (H_2O_2)-induced NAC transcription factor, as a central longevity regulator in *Arabidopsis thaliana*. *JUB1* overexpression strongly delays senescence, dampens intracellular H_2O_2 levels, and enhances tolerance to various abiotic stresses, whereas in *jub1-1* knockdown plants, precocious senescence and lowered abiotic stress tolerance are observed. A JUB1 binding site containing a RRYGCCGT core sequence is present in the promoter of *DREB2A*, which plays an important role in abiotic stress responses. JUB1 transactivates *DREB2A* expression in mesophyll cell protoplasts and transgenic plants and binds directly to the *DREB2A* promoter. Transcriptome profiling of *JUB1* overexpressors revealed elevated expression of several reactive oxygen species–responsive genes, including heat shock protein and glutathione *S*-transferase genes, whose expression is further induced by H_2O_2 treatment. Metabolite profiling identified elevated Pro and trehalose levels in *JUB1* overexpressors, in accordance with their enhanced abiotic stress tolerance. We suggest that JUB1 constitutes a central regulator of a finely tuned control system that modulates cellular H_2O_2 level and primes the plants for upcoming stress through a gene regulatory network that involves DREB2A.

INTRODUCTION

In plants, the transition from juvenility through maturation to senescence is a physiologically complex process that involves a large number of molecular and physiological events regulated by genetically determined and environmentally modified regulatory networks (e.g., Smart et al., 1995; Hinderhofer and Zentgraf, 2001; He and Gan, 2002; Gepstein et al., 2003; Buchanan-Wollaston et al., 2005; van der Graaff et al., 2006; Lim et al., 2007). Senescence is triggered by adverse environmental conditions, such as high salinity, low light intensity, drought, pathogen attack, nutrient deficiency, and other stresses (Dwidedi et al., 1979; Dhindsa et al., 1981; Bohnert et al., 1995; Balazadeh et al., 2010a, 2011). Many genes, including those that control transcription, undergo expression changes during senescence (e.g., Gepstein et al., 2003; Guo et al., 2004; Buchanan-Wollaston et al., 2005; van der Graaff et al., 2006; Balazadeh et al., 2008b; Parlitz et al., 2011). Recently, high-resolution temporal profiling of gene expression during leaf senescence in *Arabidopsis thaliana* revealed clusters of coexpressed genes and a distinct chronology of senescence-associated processes (Breeze et al., 2011). Among the transcription factors (TFs), the NAC (for NAM, ATAF1, 2, and CUC2) and WRKY families are particularly rich in senescence-regulated TFs in many plant species (Andersson et al., 2004; Guo et al., 2004; Lin and Wu, 2004; Buchanan-Wollaston et al., 2005; Gregersen and Holm, 2007; Balazadeh et al., 2008b), suggesting they play important roles in leaf senescence. Although more than 20 of the 106 known *NAC* genes in *Arabidopsis* exhibit senescence-dependent expression (and, thus, represent senescence-associated genes [SAGs]), a distinct regulatory function with respect to senescence has only been reported for some members so far, including At *NAP* (for *NAC-LIKE*, *ACTIVATED BY APETALA3/PISTILLATA*; also called *Arabidopsis NAC* [*ANAC*] *029*; Guo and Gan, 2006), *ORESARA1* (*ORE1*; *ANAC092*, At *NAC2*; Kim et al., 2009; Balazadeh et al., 2010a), and *ORESARA1 SISTER1* (*ORS1*; *ANAC059*; Balazadeh et al., 2011). Inhibiting either NAC individually delays senescence, identifying them as nonredundant positive regulators of

[1] These authors contributed equally to this work.
[2] Address correspondence to bmr@uni-potsdam.de.
The authors responsible for distribution of materials integral to the findings presented in this article in accordance with the policy described in the Instructions for Authors (www.plantcell.org) are: Bernd Mueller-Roeber (bmr@uni-potsdam.de) and Salma Balazadeh (balazadeh@mpimp-golm.mpg.de).
[W] Online version contains Web-only data.
[OA] Open Access articles can be viewed online without a subscription.
www.plantcell.org/cgi/doi/10.1105/tpc.111.090894

senescence (Guo and Gan, 2006; Kim et al., 2009; Balazadeh et al., 2010a, 2011). A dual-function NAC gene, *VASCULAR-RELATED NAC-DOMAIN INTERACTING2* (*VNI2*; *ANAC083*), was recently reported to integrate abscisic acid (ABA) signaling with leaf senescence (Yang et al., 2011) and to negatively regulate xylem vessel formation (Yamaguchi et al., 2010). Genes downstream of ORE1 and ORS1 have been identified; from these studies, it became apparent that both TFs exert their function through regulatory networks that include many known SAGs (Balazadeh et al., 2010a, 2011). Of the 170 genes upregulated after expression of *ANAC092* is induced, 102 genes were also enhanced by senescence in the time-course experiment reported by Breeze et al. (2011). The majority of these genes (75%) fell into clusters whose gene members were enriched for promoter-localized NAC binding sites. This observation supports the conclusion that ANAC092/ORE1 and most likely other NAC TFs play an important role in regulating senescence.

An apparent signaling element for the regulation of senescence is hydrogen peroxide (H_2O_2). Diverse environmental and developmental stimuli, such as heat stress, salinity, cold, and pathogen attack, are known to trigger an accumulation of intracellular H_2O_2 and through this regulate the expression of many genes, including TFs of, for example, the NAC, WRKY, and APETALA2 (AP2)/ethylene-responsive element binding protein (EREBP) families (Vanderauwera et al., 2005; Gadjev et al., 2006). Notably, the expression of at least 15 senescence-associated NAC TFs increases rapidly after H_2O_2 treatment, including, for example, At *NAP*, *ANAC092/ORE1*, *ORS1*, *ARABIDOPSIS TRANSCRIPTION ACTIVATION FACTOR1* (*ATAF1*), and *ANAC032* (Balazadeh et al., 2010b, 2011). However, the H_2O_2 and senescence-dependent gene regulatory networks of these TFs are just emerging and are far from being fully understood.

DEHYDRATION-RESPONSIVE ELEMENT BINDING PROTEIN2A (DREB2A) belongs to the EREBP family of TFs. Although *DREB2A* expression increases during senescence, its biological role in this process has not been analyzed. Expression of *DREB2A* is induced by dehydration, salinity, heat, and different oxidative stress treatments, including H_2O_2 stress (Gadjev et al., 2006; Sakuma et al., 2006a; Suzuki et al., 2011). DREB2A regulates the water deficit–inducible expression of target genes and requires posttranslational modification for its activation. Two C3HC4 RING domain-containing proteins, including DREB2A-INTERACTING PROTEIN1 (DRIP1) and DRIP2, have been discovered and shown to interact with DREB2A in the nucleus. DRIPs act as E3 ubiquitin ligases that mediate the ubiquitination of DREB2A, thereby targeting the TF to 26S proteasome degradation. DRIP1 and DRIP2 thus function as negative regulators of drought-responsive gene expression (Qin et al., 2008). Recently, Suzuki et al. (2011) identified a new heat stress regulon in *Arabidopsis* regulated by multiprotein bridging factor 1c (MBF1c). *DREB2A* is one of the 36 genes whose expression during heat stress is regulated by MBF1c, and genetic studies demonstrated that *DREB2A* is required for plant survival under heat stress (Suzuki et al., 2011). Overexpression of a constitutively active form of DREB2A (*35S:DREB2A CA*) resulted in the upregulation of nearly 500 genes, including drought- and salt-responsive genes, and also heat shock–related genes (Sakuma et al., 2006b). The heat shock TF gene *HsfA3* is a known direct target of DREB2A (Schramm et al., 2008).

Here, we report the identification of JUNGBRUNNEN1 (JUB1), a NAC TF that negatively regulates senescence. *JUB1* is rapidly and strongly induced by H_2O_2 treatment. Overexpression of *JUB1* markedly extends leaf longevity and promotes tolerance to various abiotic stresses. We found that increased tolerance to abiotic stress correlates with reduced levels of H_2O_2 in *JUB1* overexpressors, whereas the opposite is observed in *jub1-1* knockdown plants, suggesting that JUB1 participates in regulating the cellular H_2O_2 homeostasis network. We further determined the binding site of the JUB1 TF by in vitro binding site selection and discovered *DREB2A* as one of its direct downstream target genes. Thus, JUB1 links H_2O_2 signaling to senescence regulation and the downstream activation of *DREB2A* and its direct target *HsfA3*.

RESULTS

JUB1 Promotes Leaf Longevity

To identify novel transcription regulators that modulate leaf senescence, we systematically screened *NAC* gene T-DNA insertion mutants and cauliflower mosaic virus (CaMV) 35S-driven overexpression lines for extended longevity compared with wild-type *Arabidopsis* plants kept under identical growth conditions. We found that plants overexpressing *At2g43000* developed senescence considerably later than the wild type and retained fully green leaves for a much longer period (see below). By contrast, a knockdown mutant of *At2g43000* (Salk ID 036474) developed leaf senescence earlier than the Columbia-0 (Col-0) wild type (see below). Similarly, we observed earlier senescence in transgenic plants upon suppression of *At2g43000* transcript abundance by means of a genome-inserted artificial microRNA construct (see Supplemental Figure 1 online). These observations identify *At2g43000* as a novel genetic regulator of plant senescence. As elevated expression of *At2g43000* extended longevity, we designated it *JUNGBRUNNEN1* (*JUB1*; German for "Fountain of Youth").

JUB1 encodes a 275–amino acid protein of a calculated molecular mass of 31.5 kD. JUB1 contains a NAM domain (pfam02365) at its N terminus. Its coding region consists of three exons, interrupted by two introns. Phylogenetic analyses revealed the presence of *JUB1* orthologs in other plant species, including rice (*Oryza sativa*; ONAC066; Ooka et al., 2003) and *Populus trichocarpa* (PNAC080-083; Hu et al., 2010). Expression of a JUB1–green fluorescence protein (GFP) fusion in *Arabidopsis* showed its predominant accumulation in the nucleus (see Supplemental Figure 2 online), consistent with its function as a transcription regulator.

RNA gel blot analysis and quantitative RT-PCR (qRT-PCR) confirmed elevated *JUB1* transcript level in multiple independent *35S:JUB1* transformants compared with the wild type (Figures 1A and 1B). When grown in soil under long-day conditions, leaf senescence and bolting were strongly delayed in *35S:JUB1* plants compared with the wild type and empty vector (EV)–transformed control lines (Figure 1C). Overexpressors started bolting 10 to 14 d later than the EV lines. Chlorophyll levels of 12 individual rosette leaves of overexpression plants were higher than those in age-matched EV plants (Figure 1D). Mortality

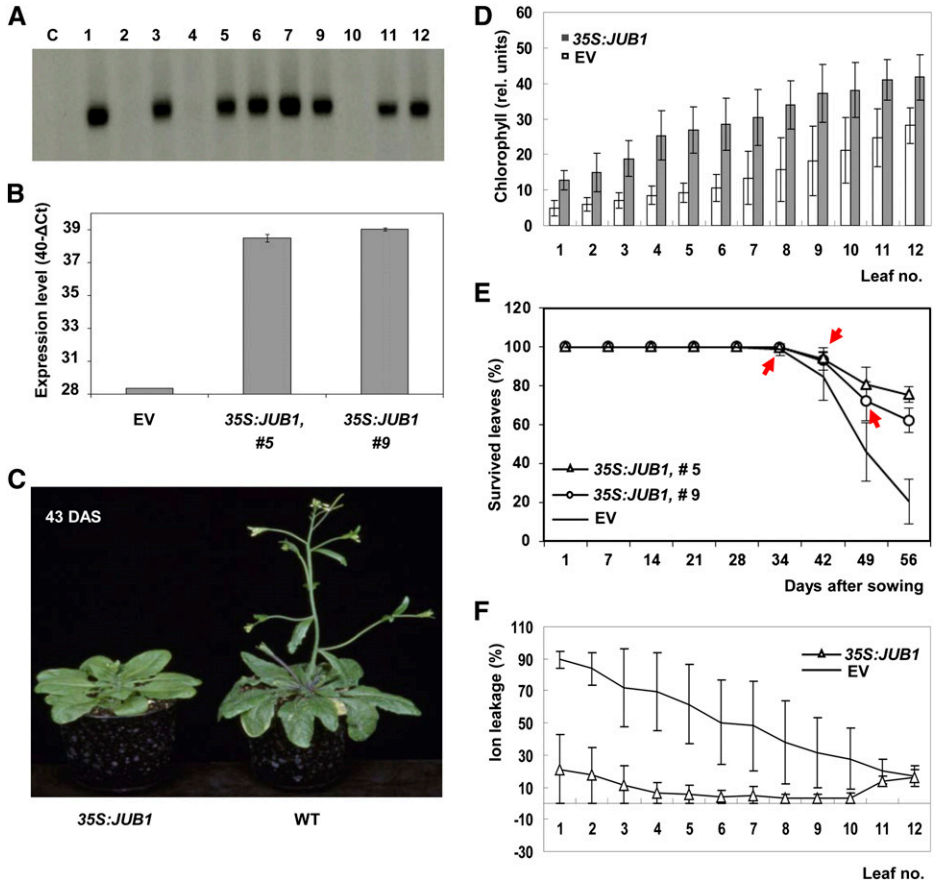

Figure 1. Physiological and Molecular Characterization of *JUB1* Overexpression Plants.

(A) RNA gel blot analysis of plants transformed with the *35S*:*JUB1* construct. Radiolabeled *JUB1* cDNA was used as hybridization probe. Numbers indicate individual transformants; C, nontransformed wild-type (Col-0) control. Elevated *JUB1* expression compared with wild-type plants is observed in transgenic lines 1, 3, 5, 6, 7, 9, 11, and 12.

(B) Increased *JUB1* expression in lines 5 and 9, as confirmed by qRT-PCR, compared with EV control.

(C) Delayed bolting in *35S*:*JUB1* overexpression line compared with the wild type (WT) at 43 d after sowing (DAS).

(D) Elevated chlorophyll content in leaves 1 to 12 of *35S*:*JUB1* overexpressors compared with EV control plants at ~60 DAS (n = 6).

(E) Percentage of survived leaves at different plant ages (given as DAS). Bolting time points are indicated by red arrows. Note steeper slope for curve of EV plants compared with *35S*:*JUB1* overexpressors between days 34 and 56 (n = 14 to 17).

(F) Ion leakage of leaves 1 to 12 of *35S*:*JUB1* and EV control plants at ~60 DAS.

Data in **(B)** and **(D)** to **(F)** are the means of at least three biological replicates ± SD.

curves confirmed later senescence in overexpressors than in EV lines (Figure 1E). In accordance with this, ion leakage as an indicator of senescence was much less pronounced in overexpression plants than in EV controls (Figure 1F). We also expressed *JUB1* from the *RD29A* promoter, which shows basal activity in nonstressed plants, but enhanced activity upon abiotic stress (Kasuga et al., 1999). We observed extended longevity, accompanied by delayed bolting, in *RD29A*:*JUB1* plants, which was dependent on *JUB1* expression level (see Supplemental Figure 3 online).

Next, we characterized a SALK T-DNA insertion line (Col-0 background). The T-DNA insertion in the second intron, 1034-bp downstream of the start codon (Figure 2A), was confirmed by PCR on genomic DNA of *jub1-1* plants (see Supplemental Figure 4 online). RT-PCR analysis revealed a reduction in *JUB1* transcript abundance in fully expanded *jub1-1* mutant leaves compared with leaves of equivalently aged wild-type plants (Figure 2B). Phenotypic analysis of the *jub1-1* mutant revealed earlier bolting than in the wild type (up to 3 d; Figure 2C). A >95% reduction of *JUB1* transcript level was detected by qRT-PCR in *jub1-1* plants (Figure 2D), which was accompanied by an earlier loss of chlorophyll (Figure 2E) and precocious senescence (Figures 2F).

As our data indicated a longevity-extending effect of elevated *JUB1* expression, we also tested its role in dark-induced senescence. Leaves were detached from 39-d-old soil-grown plants and kept for up to 6 d on moist filter paper in the dark; we observed that *35S*:*JUB1* overexpressors retained chlorophyll

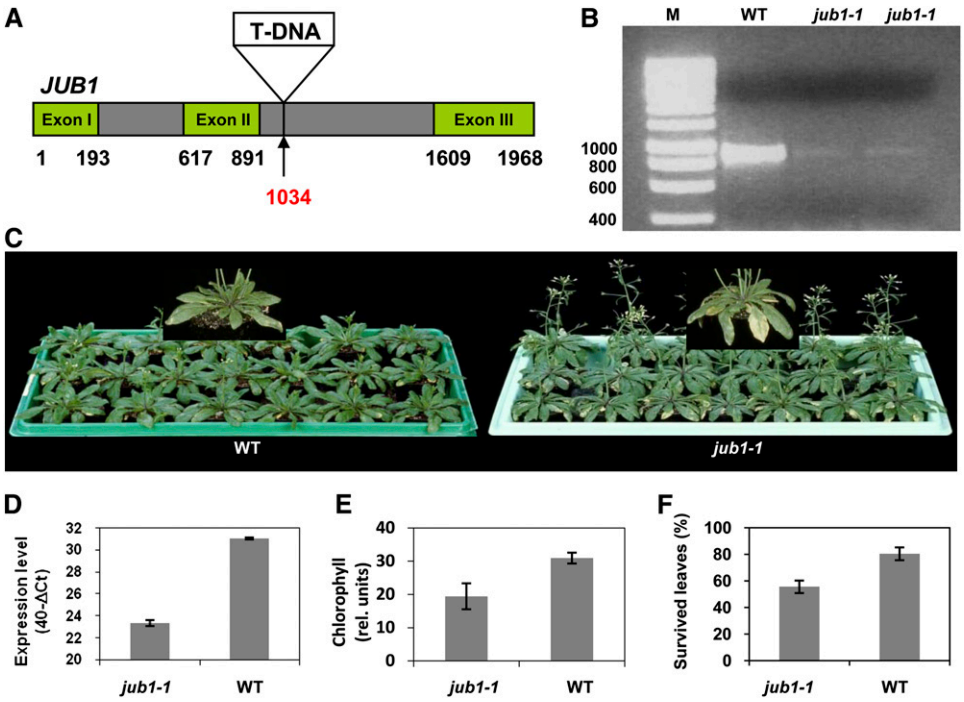

Figure 2. Physiological and Molecular Characterization of the *jub1-1* Mutant.

(A) T-DNA inserted at nucleotide position 1034 downstream of the start codon (indicated by arrow) in the second intron.
(B) Downregulation of *JUB1* transcripts in *jub1-1* mutant shown by RT-PCR with primers annealing to the start and stop regions of the coding sequence. M, molecular size marker (sizes in base pairs); WT, wild type.
(C) Comparison of *jub1-1* plants with wild-type plants at 47 DAS. Note early bolting and early senescence in the mutant plants.
(D) Downregulation of *JUB1* transcript abundance in *jub1-1* line, as confirmed by qRT-PCR.
(E) The *jub1-1* mutant contains less chlorophyll than the wild type in the five biggest leaves at 47 DAS.
(F) The *jub1-1* mutant exhibits a lower percentage of survived leaves than the wild type at 47 DAS. Data in graphs are the means of at least three biological replicates ± SD.

better than the *jub1-1* knockdown and EV control lines, reminiscent of a delay in senescence (see Supplemental Figure 5 online).

Expression Profiling of SAGs in *JUB1* Transgenic Plants

To further substantiate the role of JUB1 for the regulation of leaf senescence, we analyzed the expression of 168 SAGs (including 49 TFs) in wild-type and *JUB1*-modified plants by qRT-PCR. The SAGs included in our expression profiling platform were previously shown to be highly upregulated during natural senescence in wild-type plants (see Supplemental Data Set 1 online; Buchanan-Wollaston et al., 2005; van der Graaff et al., 2006; Balazadeh et al., 2008b; Parlitz et al., 2011). The platform included *SAG12*, a well-known senescence marker gene (Noh and Amasino, 1999). At a twofold cutoff, the expression of 89 SAGs (including 21 TFs and *SAG12*), representing ~53% of all SAGs tested, was downregulated in *35S:JUB1* plants compared with the wild type, while only six SAGs (including *JUB1*) were upregulated (see Supplemental Data Set 1 online; Figure 3A). By contrast, expression of 97 SAGs (including 19 TFs), representing ~58% of all SAGs tested here, were upregulated in *jub1-1* compared with the wild type, and only two SAGs (including *JUB1*) were downregulated in *jub1-1* plants (Figures 3B and 3C; see Supplemental Data Set 1 online). Collectively, our data support the model that JUB1 constitutes a negative regulator of leaf senescence and, hence, a driver of longevity.

Estradiol-Inducible *JUB1* Overexpression

We next tested the effect of estradiol (EST)-inducible *JUB1* expression on bolting and leaf senescence using the system described by Zuo et al. (2000). qRT-PCR revealed induction of *JUB1* expression in EST-treated *JUB1-IOE* seedlings already after 1 h of EST treatment and expression further increased at longer incubation times (Figure 4A). We sowed *JUB1-IOE* lines on half-strength Murashige and Skoog (MS) medium containing 1% Suc and 10 μM EST (or 0.1% ethanol in control experiments). After stratification at 4°C for 3 d, plates were transferred to a growth chamber at long-day conditions. Bolting was delayed in EST-treated *JUB1-IOE* plants compared with mock-treated controls (Figure 4B). When grown in liquid medium, *JUB1-IOE* seedlings remained green (nonsenescent) longer in the presence of EST (15 μM) than in mock-treated seedlings (Figure 4C). Thus, high *JUB1* expression suppressed bolting and delayed senescence under in vitro conditions, similar to plants grown in soil.

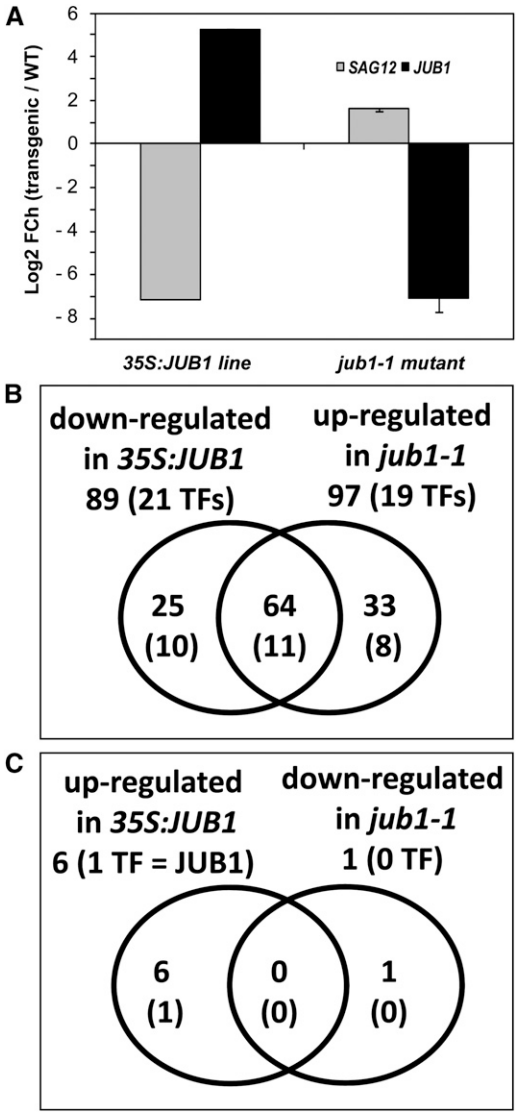

Figure 3. Transcript Profiling of SAGs.

(A) Expression of *JUB1* and the late-senescence marker gene *SAG12* in *35S*:*JUB1* and *jub1-1* plants compared with the wild type (WT) (numbers on the *y* axis indicate log2 fold-change (FCh) expression ratio compared with the wild type).

(B) and **(C)** Venn diagrams of SAGs differentially expressed in *35S*:*JUB1* and *jub1-1* plants compared with the wild type at 47 DAS. Numbers in parentheses indicate senescence-associated TFs. See also Supplemental Data Set 1 online.

Age-Dependent *JUB1* Expression

We next analyzed the *JUB1* expression pattern in *Arabidopsis* (Col-0) and tobacco (*Nicotiana tabacum* cv Samsum NN) plants transformed with a *JUB1* promoter-β-glucuronidase (GUS) reporter construct (Pro_{JUB1}:*GUS*). *JUB1* expression was observed in various tissues throughout plant development. In *Arabidopsis* seedlings, GUS activity was preferentially detected in roots, cotyledons, and the tips of young leaves. GUS staining was generally more pronounced in leaf tips and margins than the central part of the leaf blade (Figures 5A and 5B). Expression was also observed in floral tissues, preferentially in old sepals, petals, stamens, mature anthers, and pollen grains, while immature floral tissue did not show GUS activity (Figures 5C and 5D). GUS activity was also observed in the abscission zone of open flowers (data not shown). In the half expanded leaves of soil-grown plants, GUS staining was observed in the tip region only; in fully expanded leaves, strong GUS staining was observed in the senescent regions (Figures 5E and 5F). Moreover, GUS activity was detected in primary and lateral roots (Figures 5A, 5G, and

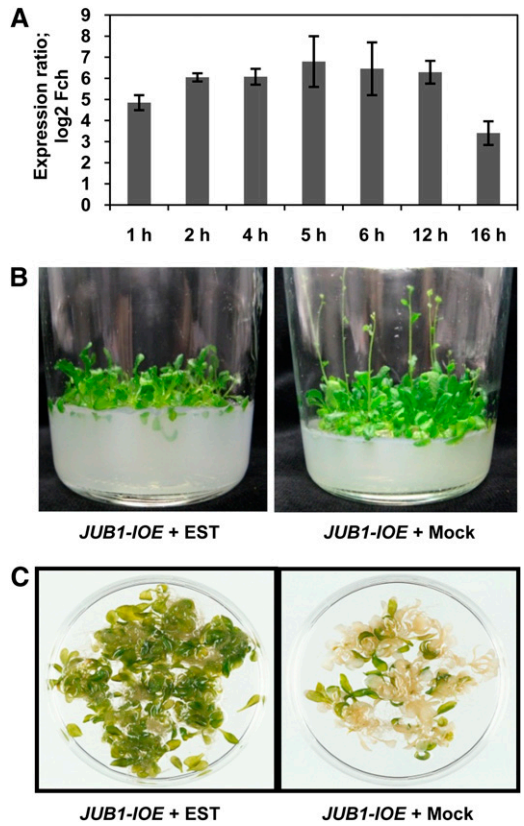

Figure 4. Phenotypic Analysis of *JUB1-IOE* Lines.

(A) *JUB1* expression is induced in leaves of *JUB1-IOE* seedlings after treatment with 10 μM EST compared with mock treatment (0.1% ethanol). Treatment times are indicated. Data are the means of three biological replicates ± SD. Fch, fold change.

(B) Induction of *JUB1* expression by EST in *JUB1-IOE* plants delays bolting when grown in vitro. Plants were grown for 6 weeks in glass jars on medium containing 10 μM EST (0.1% ethanol for control experiment). In this experiment, five independent transgenic lines were tested; the photographs shown represent a typical result.

(C) Delayed senescence in *JUB1-IOE* plants grown in vitro. Two-week-old *JUB1-IOE* seedlings were transferred to flasks with liquid medium containing 15 μM EST, or 0.15% ethanol as control, and kept on a rotary shaker (slow motion) under continuous light for 1 week. Note the delayed senescence upon *JUB1* induction. Three independent transgenic lines were used to confirm the observation made here.

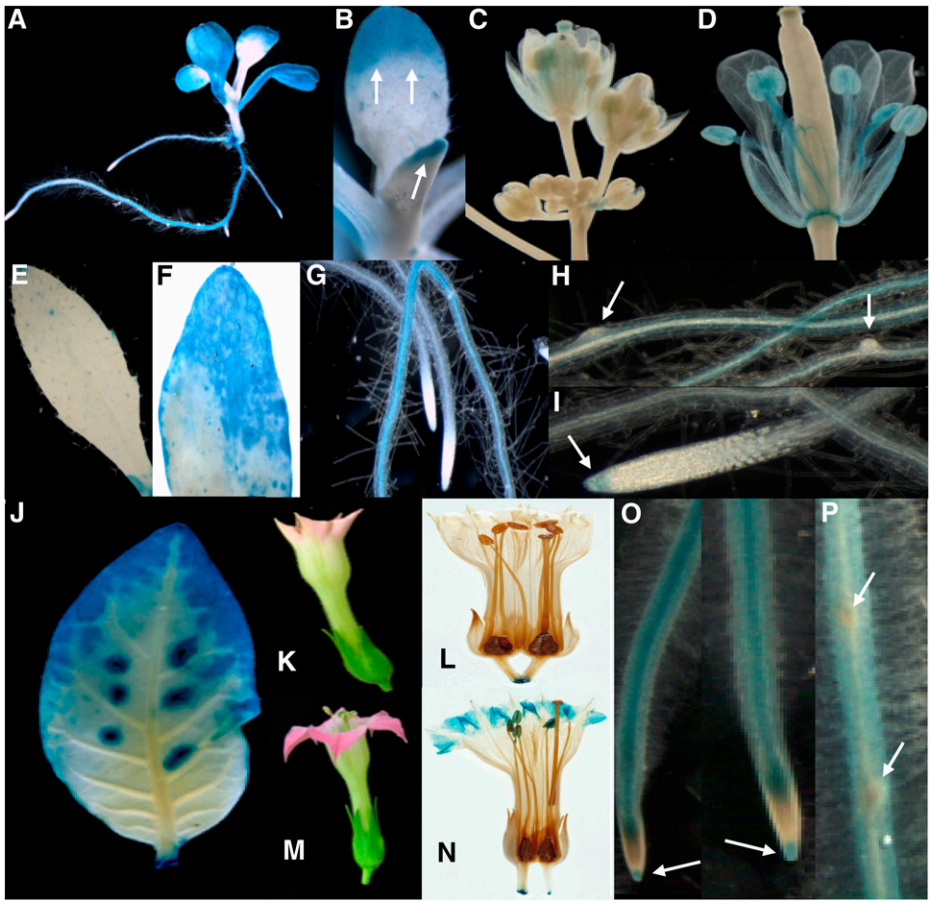

Figure 5. GUS Activity in Pro_{JUB1}:*GUS* Lines.

(A) to **(I)** *Arabidopsis*.
(A) Ten-day-old seedling. GUS staining is mainly localized to cotyledons, the tip regions and margins of leaves representing the oldest but not yet senescent leaf regions, and primary and secondary roots.
(B) Ten-day-old seedling. Strong GUS staining located in tips of newly emerging leaves (arrows).
(C) and **(D)** Flowers at different development stages. GUS staining is virtually absent in unopened young flowers. In open flowers **(D)**, GUS staining appears in mature anthers, filaments, and the stamen abscission zone.
(E) GUS staining is weak to absent in ~50% expanded leaves from soil-grown plants.
(F) Strong GUS staining is located in senescent regions of a partially senescent leaf from soil-grown plants.
(G) GUS staining in roots; note the absence of GUS activity in the meristematic zone.
(H) GUS staining is absent from emerging lateral roots (arrows).
(I) GUS staining in root cap (arrow). Staining was for ~1 h.
(J) to **(P)** Tobacco.
(J) Leaf, with more intense staining in the tip and margins. GUS activity is also visible around wound sites.
(K) and **(L)** Young flower without GUS staining.
(M) and **(N)** Open flower showing GUS staining in petal tips and anthers.
(O) Roots. Note the absence of GUS activity in the meristematic zone, whereas the root cap shows GUS staining (arrows).
(P) Absence of GUS activity from emerging lateral roots (arrows). Staining was for ~6 h.

5H), including the root cap of extended roots (Figure 5I). However, *JUB1* promoter activity was absent from cells of emerging lateral roots (Figure 5H) and from root meristematic zones that faded into the elongation zones (Figures 5G and 5I).

In transgenic Pro_{JUB1}:*GUS* tobacco leaves, GUS staining was only observed in older parts (i.e., the tips and margins), consistent with an age-dependent upregulation of *JUB1* expression (Figure 5J). No GUS staining was observed in young flowers when corolla limbs began to open (Figures 5K and 5L); however, in open flowers, intense GUS staining was evident in the tip regions of corolla limbs, but not corolla tubes. Additionally, *JUB1* promoter activity was visible in anthers (Figures 5M and 5N). Moreover, GUS staining was observed in roots (Figures 5O and 5P), including the root tip of extended, but not young, emerging roots. As in *Arabidopsis*, no *JUB1* promoter activity was detected in the root meristematic zone (Figure 5O).

H_2O_2 Triggers *JUB1* Expression

H_2O_2 plays a central role in plant signaling and stress responses. In microarray hybridization experiments, we previously observed strong induction (~25-fold) of *JUB1* transcript level in *Arabidopsis* seedlings after 5 h of exposure to 10 mM H_2O_2 (Balazadeh et al., 2010b). Here, we confirmed H_2O_2-responsive *JUB1* expression by qRT-PCR in 2-week-old *Arabidopsis* plants treated for 30 min or 2, 4, or 6 h with 10 mM external H_2O_2. *JUB1* transcript abundance increased in both whole seedlings and leaves already 30 min after treatment and increased further thereafter (Figures 6A and 6B). Similarly, *JUB1* expression increased approximately fivefold within 5 h of pharmacological inhibition of the H_2O_2-scavenging enzyme catalase in seedlings (see Supplemental Figure 6A online). In Pro_{JUB1}:*GUS* lines, enhanced GUS activity was observed 30 min or 1 h after treatment with 10 mM or 50 mM H_2O_2 (Figures 6C and 6D), indicating that the response of *JUB1* to H_2O_2 is regulated at the promoter level and mediated by one or more currently unknown upstream transcription regulators.

It was previously reported that endogenous H_2O_2 concentration rises during bolting in *Arabidopsis* leaves, and downregulation of catalase (CAT2) activity was suggested to be the initial step of this rise (Zimmermann et al., 2006). To investigate a possible correlation between the level of endogenous H_2O_2 and *JUB1* expression, we measured both H_2O_2 content and *JUB1* expression in leaves of ~35-d-old *Arabidopsis* wild-type plants at bolting (1-cm main flower stalk). Leaves number 2 (second oldest rosette leaf) to 14 were sampled individually; younger leaves were collected in groups A (>25 mm leaf length), B (15 to 25 mm), and C (below 15 mm), respectively (leaf number 1 was too old and deteriorated for measurements). *JUB1* expression was determined by qRT-PCR, and H_2O_2 level was quantified using an Amplex Red assay. We observed that endogenous H_2O_2 and *JUB1* transcript abundance followed similar patterns with higher levels in older leaves (numbers 2 to 12) than in younger leaves (numbers 13 and 14, groups A to C); particularly low H_2O_2 and *JUB1* transcript levels were present in the youngest rosette leaves (see Supplemental Figure 7 online). Thus, our data indicate that *JUB1* expression follows the level of endogenous H_2O_2 dependent on leaf age.

Various abiotic stresses, including salinity, cold, and heat stress, cause the accumulation of endogenous H_2O_2. In a microarray hybridization experiment, we observed induction of *JUB1* expression when hydroponically grown plants were subjected to salinity stress (150 mM NaCl) over a period of 4 d (see Supplemental Figure 6B online). Salt stress (150 and 200 mM NaCl) slightly induced GUS activity in Pro_{JUB1}:*GUS* plants after 24 h (4-methyl umbelliferyl β-D-glucuronide [MUG] assay; see Supplemental Figure 8A online). Several other treatments that cause an intracellular rise of H_2O_2 level induce *JUB1* expression, including treatment with cellulase R-10 (see Supplemental Figures 8B and 8C online), paraquat (methyl viologen) (see Supplemental Figures 8B and 8C online), ozone (Gadjev et al., 2006), 3-aminotriazole, which blocks the activity of the H_2O_2 scavenging enzyme catalase (Gechev and Hille, 2005), and AAL (*Alternaria alternata* fungal

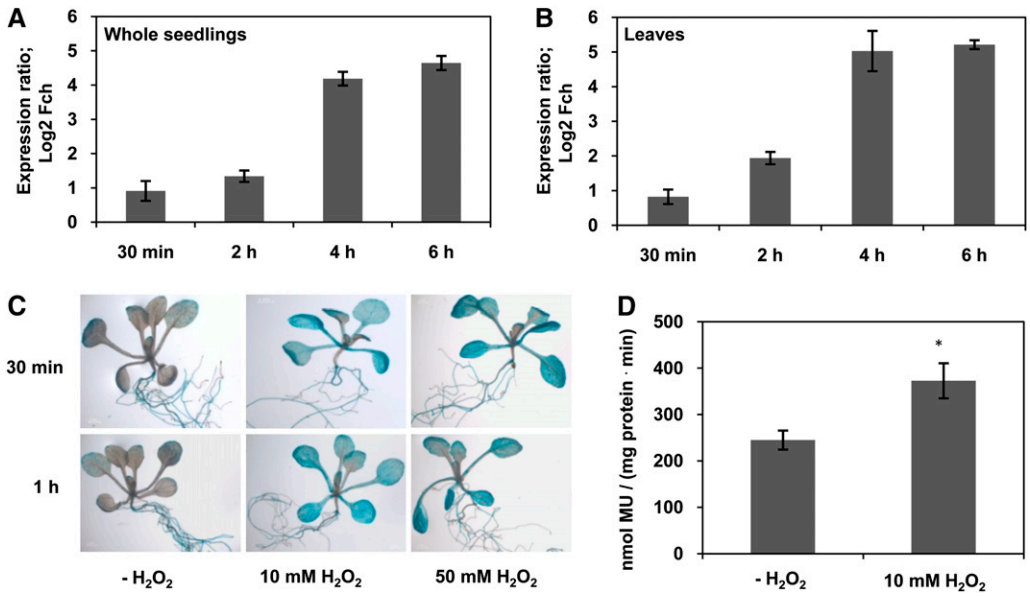

Figure 6. Effect of H_2O_2 on *JUB1* Expression.

(A) and **(B)** *JUB1* transcript level in whole seedlings **(A)** and leaves **(B)** of wild-type *Arabidopsis* plants as determined by qRT-PCR after treatment with 10 mM H_2O_2 for 30 min or 2, 4, and 6 h compared with nontreated samples.

(C) Pro_{JUB1}:*GUS* lines treated with H_2O_2. Two-week-old seedlings were transferred to medium containing 10 or 50 mM H_2O_2 and incubated for 30 min or 1 h, respectively. Elevated GUS activity was observed at both concentrations already 30 min after treatment.

(D) GUS activity of Pro_{JUB1}:*GUS* seedlings measured by a MUG assay after treatment with 10 mM H_2O_2 for 30 min. Asterisk indicates significant difference ($P < 0.05$, Student's *t* test). Data are the means of three biological replicates ± SD. MU, methylumbelliferone.

toxin that induces H_2O_2 accumulation and cell death through perturbation of sphingolipid metabolism; Gechev and Hille, 2005). Collectively, these data indicate that *JUB1* expression is triggered by an intracellular rise of H_2O_2 level.

Overexpression of *JUB1* Enhances Tolerance to Salt Stress

Salt stress triggers the accumulation of intracellular H_2O_2 (e.g., Chung et al., 2008). To investigate whether overexpression of *JUB1* enhances tolerance to salt stress, the effect of 150 mM NaCl on *JUB1-IOE* and *jub1-1* knockdown mutants was studied. To this end, 2-week-old *jub1-1* mutant and *JUB1-IOE* seedlings were transferred from solid MS medium to liquid MS medium containing 150 mM NaCl. In the case of *JUB1-IOE* lines, 15 μM EST was added to induce *JUB1* expression, and, as a control, 0.15% ethanol was used. All seedlings were incubated on a shaker in a growth chamber with continuous light; after 3 d of stress, the *JUB1-IOE* plants incubated in saline medium containing EST retained fivefold higher levels of chlorophyll than the plants incubated in saline medium in the absence of EST (Figures 7A and 7B). By contrast, chlorophyll content in *jub1-1* seedlings was only half that of wild-type plants when stressed by salt (Figures 7C and 7D).

JUB1 Enhances Tolerance to H_2O_2 by Regulating Its Cellular Concentration

Similar to findings in animals, extended life span in plants has been observed to be closely related to increased tolerance to oxidative stress. In particular, several *Arabidopsis* mutants with extended longevity have been shown to exhibit superior tolerance to oxidative stress. Examples include transgenic plants overexpressing the *CBF2* and *CBF3* TFs, the *ore1*, *ore3*, and *ore9* mutants, and the very late flowering, long-living mutant *gigantea* (Kurepa et al., 1998; Woo et al., 2004; Sharabi-Schwager et al., 2010). The *gigantea* mutant exhibits enhanced tolerance to various types of oxidative stress, such as paraquat- and H_2O_2-induced oxidative stress (Kurepa et al., 1998).

To determine whether there is a link between increased *JUB1* expression and enhanced tolerance to oxidative stress, we first analyzed the effect of H_2O_2 treatment on *JUB1* transgenic plants.

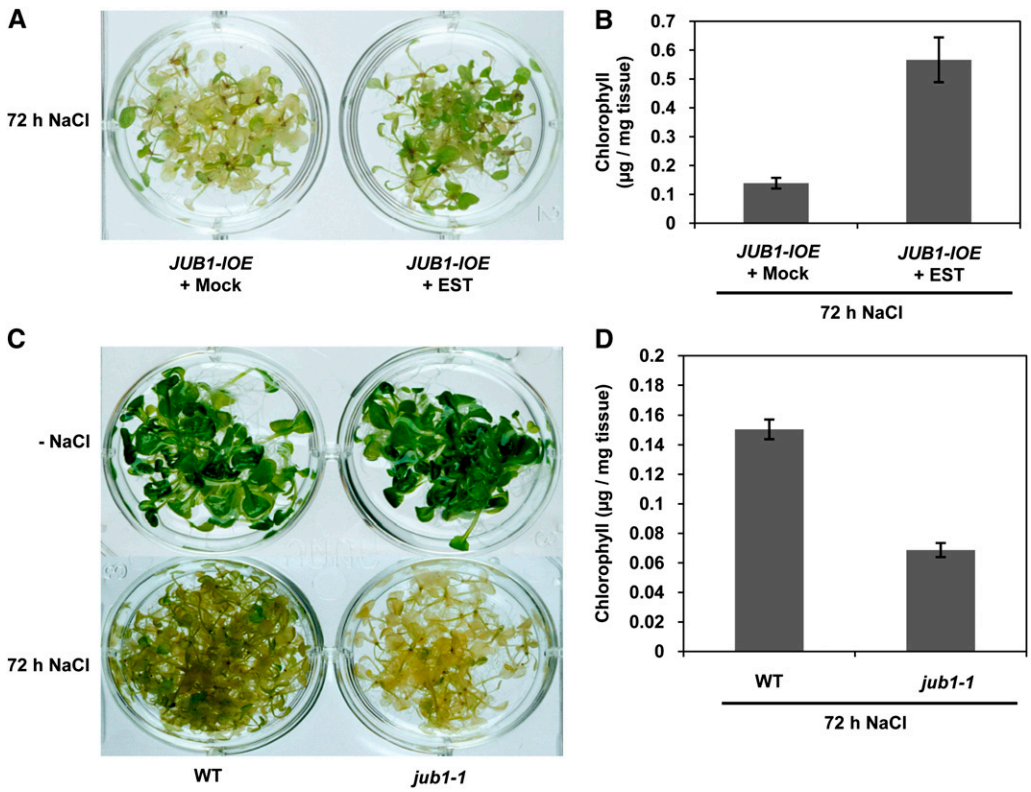

Figure 7. EST-Treated *JUB1-IOE* Plants Exhibit Increased Tolerance to NaCl Stress, Whereas Tolerance to NaCl Is Reduced in the *jub1-1* Mutant.

(A) Two-week-old *JUB1-IOE* seedlings were transferred from solid MS medium to liquid MS medium containing 150 mM NaCl, in the absence (mock; 0.15% ethanol) or presence of 15 μM EST added to induce *JUB1* expression. Plants were incubated for 72 h. EST-treated *JUB1-IOE* seedlings are more tolerant to salt stress.

(B) Higher chlorophyll levels are retained in EST-treated *JUB1-IOE* seedlings after salt treatment.

(C) Seedlings of wild-type (WT) plants are less affected by 72 h salt treatment (150 mM NaCl) than those of the *jub1-1* mutant.

(D) Chlorophyll content remains higher in the wild type (WT) than *jub1-1* plants after stress treatment. Data in **(B)** and **(D)** are the means of three biological replicates ± SD.

Two-week-old *RD29A*:*JUB1* seedlings were treated with 10 mM H_2O_2. As shown in Figure 8A, seedlings subjected to treatment for 24 h retained chlorophyll more efficiently than EV-transformed control plants. Additionally, we cultured *35S*:*JUB1* and EV seedlings on sterile medium containing 0 or 10 mM H_2O_2. *35S*:*JUB1* plants remained healthier and showed less leaf bleaching in the presence of H_2O_2 than the control line (data not shown). We next tested H_2O_2 tolerance of *JUB1-IOE* lines by transferring 3-week-old seedlings from half-strength solid MS medium to fresh medium containing 15 μM EST and 10 mM H_2O_2; control seedlings were similarly treated with H_2O_2, but EST was omitted (mock treatment: 0.15% ethanol). After 6 d, the *JUB1-IOE* plants treated with H_2O_2 and EST were more vital than plants treated with H_2O_2 alone (Figure 8B). We next tested the effect of reduced *JUB1* expression on H_2O_2 tolerance. Leaves detached from 35-d-old soil-grown *jub1-1* and EV plants were incubated in 10 mM H_2O_2 for 5 d; EV leaves remained greener than those of the *jub1-1* mutant (see Supplemental Figures 9A and 9B online). Moreover, when 12-d-old seedlings were incubated in MS medium with 10 mM H_2O_2 for 6 h tissue damage was more prominent in *jub1-1* than wild-type seedlings. Accordingly, diaminobenzidine (DAB) staining revealed a higher H_2O_2 accumulation in *jub1-1* than wild-type plants (Figure 9A). We confirmed a slight (~14%) but significant increase in H_2O_2 concentration in 12-d-old *jub1-1* seedlings compared with the wild type using an Amplex Red assay (Figure 9B). Next, we tested the effect of elevated *JUB1* expression on cellular H_2O_2 level. To this end, we treated *JUB1-IOE* lines in the absence (control) or presence of 15 μM EST (to induce *JUB1* expression) with 10 mM H_2O_2 for 6 h and observed that EST-treated seedlings accumulated slightly less (~10%) H_2O_2 than the controls (Figures 9C and 9D). Jointly these data indicate that JUB1 counteracts the cellular accumulation of H_2O_2.

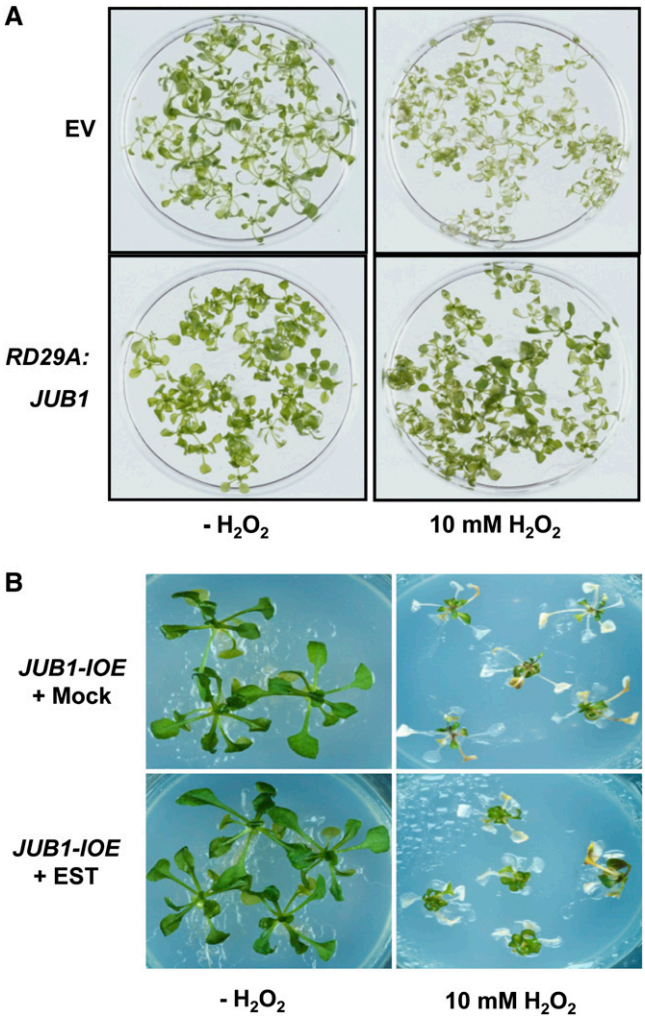

Figure 8. Overexpression of *JUB1* Confers Tolerance to H_2O_2.

(A) Two-week-old *RD29A*:*JUB1* and EV seedlings grown on solid MS medium were transferred to liquid medium containing 10 mM H_2O_2 and incubated for 24 h. *RD29A*:*JUB1* seedlings remained green, whereas EV lines bleached in the presence of H_2O_2.

(B) *JUB1-IOE* lines treated with 15 μM EST survived better than plants treated with 0.15% ethanol (mock treatment) after transferring 3-week-old plants to fresh medium containing 10 mM H_2O_2 for 6 d.

A Heat Shock Protein Response Network Regulated by JUB1

To start unraveling the H_2O_2 regulatory network regulated by JUB1, we tested the expression of 187 reactive oxygen species (ROS)–responsive genes in 2-week-old seedlings of *RD29A*:*JUB1* and *jub1-1* plants before and after treatment with H_2O_2 (10 mM, 6 h) and compared results with data from wild-type seedlings. Expression analysis was performed by qRT-PCR. Genes included in the ROS expression platform are known to be induced by H_2O_2, superoxide anion, and/or singlet oxygen (for details, see Methods) and encode TFs, heat shock proteins (HSPs), protein kinases, glutathione *S*-transferases (GSTs), and others (see Supplemental Data Set 2 online).

Our data revealed detectable expression of 179 ROS genes in all samples at both control and treatment conditions. We observed that expression of 36 genes was more strongly induced by H_2O_2 in *RD29A*:*JUB1* than wild-type seedlings, while expression of these genes was either not or only marginally affected by H_2O_2 treatment in *jub1-1* seedlings compared with the wild type (Table 1). These genes therefore represent prime candidates for ROS-responsive genes regulated by JUB1 during H_2O_2 signaling. Genes encoding HSPs constitute the largest fraction of the genes in the regulatory network. Upon H_2O_2 treatment, 14 *HSP* genes were more strongly induced in *RD29A*:*JUB1* seedlings compared with the wild type, whereas their expression was not or only marginally induced in *jub1-1* plants (Table 1). In addition to *HSPs*, several GST genes (including *GST10*, *24*, and *25*), TFs (e.g., *DREB2A*, *DREB2B*, *ANAC047*, and *ANAC055*), and some heat shock binding proteins were also among the ROS genes induced by H_2O_2 treatment in *RD29A*:*JUB1* transgenic plants. In accordance with the reduced induction of *HSPs* after stress in *jub1-1* seedlings, we observed a reduced heat stress tolerance (45°C, 5 h) of *jub1-1* seedlings relative to the wild type (see Supplemental Figure 10 online), whereas overexpression of *JUB1* enhanced tolerance to heat stress (see Supplemental Figure 11 online).

Collectively, our data indicate that JUB1 is a key regulator of plant stress responses. Under stress, JUB1 regulates expression

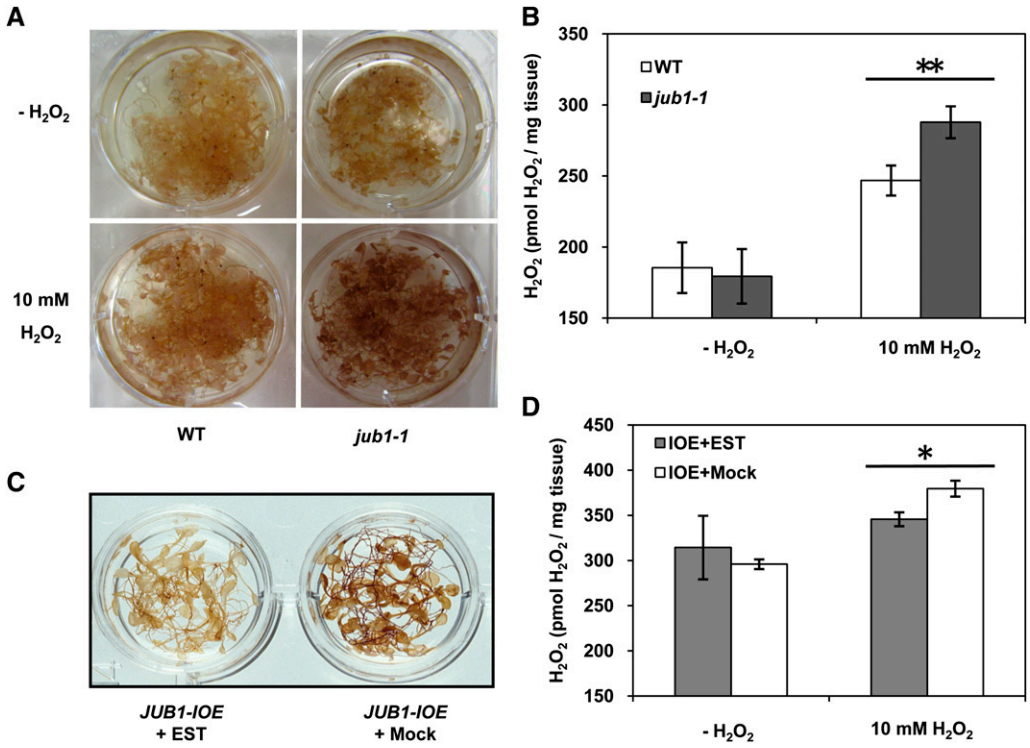

Figure 9. Overexpression of *JUB1* Reduces Endogenous H_2O_2 Content, While the Opposite Is Observed in the *jub1-1* Mutant.

(A) DAB staining of wild-type (WT) and *jub1-1* seedlings treated with 10 mM H_2O_2 for 6 h. Note the stronger DAB staining in *jub1-1* seedlings in the presence of H_2O_2.

(B) Amplex Red assay. Note the higher H_2O_2 level in H_2O_2-treated *jub1-1* seedlings compared with the wild type. Asterisks indicate significant difference ($P < 0.001$).

(C) DAB staining. *JUB1-IOE* seedlings treated with EST for 6 h accumulate less H_2O_2 than mock-treated seedlings.

(D) Amplex Red assay. Note the reduced H_2O_2 level in EST-treated *JUB1-IOE* seedlings compared with mock-treated plants (asterisk indicates significant difference; $P < 0.02$). Data in **(B)** and **(D)** are the means of three independent biological replicates ± SD.

of a set of stress tolerance genes in transgenic *Arabidopsis*, thereby leading to improved stress tolerance.

JUB1 Binding Site

To identify *cis*-elements recognized by the JUB1 TF, we performed in vitro binding site selection using the CELD-TF fusion method (Xue, 2002, 2005). Thirty-six unique double-stranded oligonucleotides bound by JUB1-CELD fusion protein were recovered after five rounds of selection using biotin-labeled double-stranded oligonucleotides containing a 30-nucleotide random sequence and were analyzed for binding activity (Table 2). Alignment of the target sequences identified RRYGCCGT as the JUB1 consensus core binding sequence. Notably, all JUB1-selected motifs, except for pf17d127, had a fixed distance to the primer sequence flanking the 30-nucleotide random sequence, indicative of primer sequences establishing part of the JUB1 recognition site. To identify nucleotide positions required for efficient JUB1 binding, and to discover potential secondary motifs contributing to JUB1 binding, nucleotide substitution experiments were performed using the sequences of selected oligonucleotides, F15d64 and F17d127, as a starting point. This analysis demonstrated that the JUB1 binding sequence consists of two elements (Table 3). We observed at least two types of sequences that differ in their 3′ parts: TGCCGT(7N)ACG and TGCCGT(7N)CCGC (N, any nucleotide). However, the second element is not essential for JUB1 binding but increases binding affinity.

DREB2A Is a Direct Target of JUB1

One of the genes induced by H_2O_2 in *RD29A*:*JUB1* seedlings that attracted our attention was *DREB2A*, a member of the AP2/EREBP TF family whose function with respect to plant responses to various abiotic stresses, such as cold and drought, is well established (Sakuma et al., 2006a, 2006b). *DREB2A* was approximately fivefold more induced by H_2O_2 in the *RD29A*:*JUB1* overexpressor than wild-type seedlings (Table 1). However, enhanced expression of *DREB2A* in *JUB1* overexpressors was also observed in the absence of H_2O_2 treatment. We found that *DREB2A* expression was elevated by more than threefold in 35-d-old *35S*:*JUB1* plants compared with wild-type plants (Figure 10A). By contrast, reduced *DREB2A* expression (~1.7-fold decrease) was observed in the *jub1-1* mutant when compared with the wild type. We also tested *DREB2A* expression in

Table 1. Genes Affected by H_2O_2 Treatment

		H_2O_2 Treatment versus Control		
		RD29A:*JUB1*/Wild Type	*jub1-1*/Wild Type	
		log2 FCh		
AGI	Description	A	B	A-B
AT1G74310	**HOT1_HSP101; ATP binding/ATPase/ nucleoside-triphosphatase/nucleotide binding**	4.69	0.99	3.70
AT2G29500	**17.6-kD Class I small HSP (HSP17.6B-CI)**	3.57	0.05	3.52
AT4G25200	**ATHSP23.6-mitochondrial small HSP23.6**	3.62	0.45	3.17
AT5G12030	**HSP17.6; unfolded protein binding**	3.98	0.97	3.01
AT1G74590	GST TAU10 (ATGSTU10_GSTU10)	2.69	−0.22	2.90
AT1G53540	**17.6-kD Class I small HSP (HSP17.6C-CI) (AA 1-156)**	3.16	0.26	2.89
AT1G71000	HSP binding	3.87	1.09	2.78
AT2G28210	ALPHA CARBONIC ANHYDRASE2 (ACA2)	2.82	0.29	2.53
AT3G09350	Armadillo/β-catenin repeat family protein	3.36	0.83	2.53
AT5G51440	**23.5-kD mitochondrial small HSP (HSP23.5-M)**	3.54	1.03	2.51
AT5G12020	**17.6 KDA CLASS II HSP (HSP17.6II)**	2.94	0.42	2.51
AT3G12580	**HSP70; ATP binding**	3.43	0.92	2.51
AT5G52640	**ATHS83_HSP81-1_HSP81.1_HSP83__ATHSP90.1; ATP binding/unfolded protein binding**	3.55	1.05	2.50
AT3G24500	ATMBF1C__MBF1C; DNA binding/transcription coactivator/TF	3.48	1.04	2.44
AT5G64510	Unknown protein	3.19	0.77	2.42
AT3G46230	**ATHSP17.4**	2.54	0.13	2.41
AT1G17170	GST TAU24 (GST_ATGSTU24)	2.34	−0.05	2.39
AT5G48570	Peptidyl-prolyl *cis-trans* isomerase, putative/FK506 binding protein	3.26	0.91	2.35
AT1G54050	**17.4-kD Class III HSP (HSP17.4-CIII)**	3.27	0.92	2.35
AT4G12400	Stress-inducible protein, putative	3.09	0.83	2.26
AT1G07160	Protein phosphatase 2C, putative/PP2C, putative	1.50	−0.70	2.20
AT2G46240	ATBAG6__BAG6; calmodulin binding/protein binding	2.61	0.43	2.18
AT2G38340	AP2 domain-containing TF, putative (DRE2B)	1.83	−0.34	2.17
AT2G26150	**HSFA2__ATHSFA2; DNA binding/TF**	3.73	1.59	2.14
AT5G05410	DREB2A; DNA binding/transcription activator/TF	2.28	0.15	2.13
AT2G32120	**HSP70T-2; ATP binding**	2.47	0.34	2.13
AT3G04070	ANAC047; TF	1.96	−0.14	2.10
AT2G20560	DNAJ heat shock family protein	3.23	1.19	2.04
AT4G37370	CYP81D8; electron carrier/heme binding/iron ion binding/monooxygenase/oxygen binding	1.93	−0.02	1.94
AT4G34410	REDOX RESPONSIVE TRANSCRIPTION FACTOR1 (RRTF1)	1.41	−0.53	1.94
AT1G17180	GST TAU25 (ATGSTU25)	2.71	0.91	1.80
AT1G16030	**Hsp70b; ATP binding**	2.27	0.48	1.79
AT3G15500	ATNAC3__ANAC055; TF	1.51	−0.12	1.63
AT3G28210	PMZ; zinc ion binding	1.66	0.06	1.60
AT4G37990	ATCAD8_CAD-B2__ELICITOR-ACTIVATED GENE 3-2 (ELI3-2); aryl-alcohol dehydrogenase/mannitol dehydrogenase	0.30	−1.29	1.58
AT1G14200	Zinc finger (C3HC4-type RING finger) family protein	1.77	0.21	1.56

Genes highly induced by H_2O_2 treatment (6 h) in the *RD29A*:*JUB1* line but either not or marginally affected in the *jub1-1* mutant when compared to wild-type plants. A threefold change (log2 = 1.5) was selected as threshold. HSPs are indicated in bold. AGI, Arabidopsis Genome Initiative; FCh, fold change.

2-week-old *JUB1-IOE* seedlings shortly (~3 h) after EST treatment. *DREB2A* expression was almost fourfold induced in the EST-treated lines, suggesting *DREB2A* as a JUB1 target gene (Figure 10A). Notably, the *DREB2A* promoter harbors a perfect match to the full JUB1 binding sequence (TGCCGTNNNNNNNNACG) ~1 kb upstream of its translation start site.

To provide further evidence for regulation of *DREB2A* by JUB1, we performed luciferase-based transactivation assays in *Arabidopsis* mesophyll cell protoplasts using the ~1.8-kb *DREB2A* promoter (including the JUB1 binding site) fused to the firefly luciferase reporter. JUB1 significantly transactivated the 1.8-kb *DREB2A* promoter (Figure 10B).

Table 2. JUB1-Selected Binding Sequences

JUB1-Selected Oligonucleotide (5′/3′)		JUB1 RBA
Bio-RS-Oligo 1		
Pf15d21	TCCCAATAGGATTCGTAA**AGTGCCGT**GTTCcgtccgccagcgcacc	0.82
Pf15d30	AGCGAAGGATCAATTGAA**GACGCCGT**GATCcgtccgccagcgcacc	0.74
Pf15d25	AATTTGACGTCATATTCT**AACGCCGT**AGTCcgtccgccagcgcacc	0.83
Pf15d64	CAACATGAAGCTA**GATGCCGT**AGACcgtccgccagcgcacc	1.18
Bio-RS-Oligo 2		
Pf16d41	TCACCCCCCCTTCTGAGGAACTC**GGTGCCGT**TCCTTTCcgtccacctgcag	0.85
Pf16d43	CCTGTGACTTTCTCGAATCATG**AGTGCCGT**GCTCTCTCcgtccacctgcag	0.48
Pf16d44	AGCGTATTCCCACTCCCGCTATG**AGTGCCGT**GCCCCCCcgtccacctgcag	0.87
Pf16d48	TGCGAACCTTGTAGTGCTCCAG**GATGCCGT**ACACCCCcgtccacctgcag	0.84
Pf16d82	ATACTTTCCCCGAGTGTGATCG**GGTGCCGT**GCTCCCCcgtccacctgcag	0.96
Pf16d84	CCATTTCGCCTTGCTGATTGCGC**GGTGCCGT**GTATCTCcgtccacctgcag	0.96
Pf16d88	AAGCATTATCGTTGTTAAATAC**GGTGCCGT**GTTCTGGCcgtccacctgcag	0.66
Pf16d98	GGGCGGGCTGGTCTCGTATTGA**GATGCCGT**ACTTGCCcgtccacctgcag	0.92
Pf16d100	CCGATATCCTGTGAACTCAGCAA**GATGCCGT**CGTCCCCcgtccacctgcag	0.89
Pf16d102	TTGGTGGTGCACGTATTTGATAG**GGTGCCGT**GTGTTCCcgtccacctgcag	0.90
Pf16d104a	ATGTTCGGCTGGATCTATATCAC**GATGCCGT**GCGTTGCcgtccacctgcag	1.20
Pf16d106	CCAATTCCCTTTTGCTGTTTAGT**AGTGCCGT**GCTGTCCcgtccacctgcag	1.01
Bio-RS-Oligo 3		
Pf17d51	GGGACTTGTATACCTGTAA**GGTGCCGT**ACCtcatgcggtacccacgtc	0.87
Pf17d52b	GGGAGGCCTCGTGCCAACC**AGTGCCGT**ACGtcatgcggtacccacgtc	1.07
Pf17d54	ACGTGATACACGCTCTATC**AGTGCCGT**GCCtcatgcggtacccacgtc	0.85
Pf17d57	AG**GCCGT**TAAACATACATG**AGTGCCGT**ACGtcatgcggtacccacgtc	1.06
Pf17d58	ACACAATTGTGACGCGAAA**GGTGCCGT**ACAtcatgcggtacccacgtc	1.02
Pf17d112	CATCGGTTTCGGCCTTGTA**GGTGCCGT**ACCtcatgcggtacccacgtc	0.94
Pf17d114	TCCGTCCTCCGAGGATCAT**GATGCCGT**ACGtcatgcggtacccacgtc	0.77
Pf17d115	TCAGGTACAACTCTGATGC**AGTGCCGT**ACCtcatgcggtacccacgtc	0.91
Pf17d116	CGAGCGTGGCCCAAAACAC**GGTGCCGT**ACCtcatgcggtacccacgtc	0.94
Pf17d117	TCAGCTTGGCTGGAGCTAG**GATGCCGT**GGGtcatgcggtacccacgtc	0.72
Pf17d118	GATCCCCCTCCTTGCCTCT**AGTGCCGT**ACCtcatgcggtacccacgtc	0.86
Pf17d120	TTCCCAGAACCTCTAACTG**GATGCCGT**ACCtcatgcggtacccacgtc	0.86
Pf17d121	GTACTA**GATGCCGT**ACGtcatgcggtacccacgtc	0.84
Pf17d124	AATGTCACTGTCCCCCTAC**AGTGCCGT**GGCtcatgcggtacccacgtc	0.91
Pf17d126	GGCTTAACCCGACAGCACA**GACGCCGT**GCCtcatgcggtacccacgtc	0.94
Pf17d127	TGCCC**AATGCCGT**GTGTAGCACGCTGCCCA	1.00
Pf17d128	AAATCCTTGTAAATCCCTA**GATGCCGT**ACTtcatgcggtacccacgtc	0.86
Pf17d129	GGTCGCACATCTCATCATG**GATGCCGT**ACCtcatgcggtacccacgtc	0.81
Pf17d130	ACGCACGTGTCTAGTATTG**AGTGCCGT**GCAtcatgcggtacccacgtc	0.99

Thirty-six JUB1-selected oligonucleotides were obtained after five rounds of in vitro DNA binding site selection. Relative binding activity (RBA) of JUB1 to oligonucleotide Pf17d127 is set to 1. Values are based on a single assay. Nucleotides in lowercase letters are from flanking primer sequences. The JUB1 core binding sequence is in bold.

We next performed an electrophoretic mobility shift assay (EMSA) to test the physical interaction of JUB1 with the *DREB2A* promoter. As shown in Figure 10C, JUB1 interacts with a 40-bp *DREB2A* promoter fragment harboring the JUB1 binding site. Finally, we used chromatin immunoprecipitation–quantitative PCR (ChIP-qPCR) to demonstrate that JUB1 binds also in vivo to the *DREB2A* promoter (Figure 10D). Thus, our data demonstrate that JUB1 is an upstream transcriptional regulator of *DREB2A*.

Metabolite Profiling Reveals Accumulation of Trehalose and Pro in *JUB1* Overexpressors

Next, we were interested to know how overexpression of JUB1 affects metabolism of the corresponding plants. Therefore, the profile of primary metabolites in rosette leaves was compared between wild-type and *JUB1* overexpression lines (*35S*:*JUB1* and *RD29A*:*JUB1*). Metabolic profiling by gas chromatography coupled to mass spectrometry (GC-MS) was performed on extracts from rosette leaves of 35-d-old plants (Figure 11A) and metabolic profiles were compared (Figure 11B). A total of 51 metabolites of known chemical structure were accurately quantified in every chromatogram. These compounds mostly included amino acids, carbohydrates (sugars and sugar alcohols), and organic acids. Overall, 67% (34 out of 51) and 55% (28 out of 51), respectively, of the identified metabolites revealed a significant difference (*$P < 0.05$, Student's *t* test) when *35S*:*JUB1* and *RD29A*:*JUB1* metabolite profiles were compared with the wild type (for an overview, see Figure 11C and Supplemental Data Set 3 online). Metabolite profiles of the two types of overexpression plants were highly similar to each other: of the 19 metabolites upregulated in *35S*:*JUB1* plants, 15 were also elevated in *RD29A*:*JUB1* plants. Similarly, of the 15 metabolites downregulated in *35S*:*JUB1* plants, six were also reduced in *RD29A*:*JUB1* plants compared with the wild

Table 3. Base Substitution or Insertion Analysis of JUB1 Binding Motifs

Synthetic Oligonucleotide Probe		JUB1 RBA
F17d127	TGCCCAA**TGCCGT**GTGTAGC**ACG**CTGCCCA	1.00 ± 0.03
F17d127m8	TGCCCTT**TGCCGT**GTGTAGC**ACG**CTGCCCA	0.82 ± 0.05
F17d127m7	TGCCCAA**AACCGT**GTGTAGC**ACG**CTGCCCA	0.46 ± 0.02
F17d127m1	TGCCCAA**TGAAGT**GTGTAGC**ACG**CTGCCCA	0.23 ± 0.01
F17d127m3	TGCCCAA**TGCCAA**GTGTAGC**ACG**CTGCCCA	0.07 ± 0.01
F17d127m9	TGCCCAA**TGCCGT**TTGTAGC**ACG**CTGCCCA	0.96 ± 0.02
F17d127m13	TGCCCAA**TGCCGT**GAATAGC**ACG**CTGCCCA	1.00 ± 0.07
F17d127m14	TGCCCAA**TGCCGT**GTGAAGC**ACG**CTGCCCA	1.02 ± 0.04
F17d127m10	TGCCCAA**TGCCGT**GTGTTTC**ACG**CTGCCCA	1.10 ± 0.02
F17d127m17	TGCCCAA**TGCCGT**GTGTAGA**ACG**CTGCCCA	1.02 ± 0.07
F17d127m4	TGCCCAA**TGCCGT**GTGTAGT**TCG**CTGCCCA	0.49 ± 0.01
F17d127m2	TGCCCAA**TGCCGT**GTGTAGC**AAA**CTGCCCA	0.56 ± 0.02
F17d127m5	TGCCCAA**TGCCGT**GTGTAGC**ACGA**AGCCCA	0.92 ± 0.05
F17d127m15	TGCCCAA**TGCCGT**GTGTAGC**ACG**CTAACCA	1.05 ± 0.06
F17d127m6f	TGCCCAA**TGCCGT**GTGTAGC**ACG**CTGTTCA	1.06 ± 0.04
F17d127m11	TGCCCAA**TGCCGT**GTGAAATAGC**ACG**CTGCCCA	0.08 ± 0.01
F17d127m12	TGCCCAA**TGCCGT**GTGTAC**AAAA**C**AAA**CCA	0.19 ± 0.02
F17d127m18[a]	TGCCCAA**TGCCGT**GTG***AAAACCGCCAGC***CA	1.01 ± 0.02
F15d64	AGCTA**GATGCCGTA**GACCGT**CCGCCAGC**GC	0.84 ± 0.02
F15d64m1	AGCTA**GATGCCGTA**GACCGT**AAGCCAGC**GC	0.45 ± 0.05
F15d64m2	AGCTA**GATGCCGTA**GACCGTCC**AACAGC**GC	0.35 ± 0.02
F15d64m3	AGCTA**GATGCCGTA**GACCGTCC**GCATGC**GC	0.59 ± 0.01
F15d64m4	AGCTA**GATGCCGTA**GACCGTCC**GCCAAA**GC	0.73 ± 0.04

Nucleotides of motif 1 and motif 2 of the JUB1 binding site are shown in bold. Mutated nucleotides are underlined. Values are means ± SD of three replicated assays. RBA, relative binding activity.

[a]Nucleotides shown in italics in F17d127m18 are derived from the flanking primer sequence of Pf15d64 (see Table 2).

type (Figure 11B). In general, the content of the major organic acids increased in the overexpression lines compared with the wild type. Among these, the level of glyceric acid and various tricarboxylic acid cycle intermediates, fumaric acid, malic acid, citric acid, and succinic acid, significantly increased in the *35S*:*JUB1* line compared with wild-type plants. Most of these components were just slightly increased in *RD29A*:*JUB1* plants. Shikimic acid content was significantly higher in both types of overexpression plants. Our data revealed that the most drastic changes were detectable in amino acids and carbohydrates. For example, among amino acids, a significant increase was observed for Pro and 4-hydroxy-Pro levels in both overexpression plants. Polyamines and compatible osmolytes, such as Pro, are known to be involved in the plant's responses to various environmental stresses, including osmotic and salt stress, heat stress, drought, cold, and pathogen infection (e.g., Yoshiba et al., 1997; Bhatnagar-Mathur et al., 2008; Verbruggen and Hermans, 2008; Gill and Tuteja, 2010). Among the detected disaccharides, the proportion of Suc significantly increased in both overexpression lines compared with the wild type. Moreover, a significant increase in the level of trehalose was observed in both overexpression lines. Trehalose is a nonreducing disaccharide of Glc that functions as an osmoprotectant (Müller et al., 1995) and stabilizes biological structures under abiotic stress conditions in bacteria, fungi, and invertebrates (Djilianov et al., 2005). Among the sugar alcohols, the levels of maltitol, glycerol (a compatible osmolyte), and erythritol were significantly higher in both overexpression lines, and the level of *myo*-inositol was significantly decreased in these lines compared with the wild type. In general, it appears that *JUB1* overexpressors accumulate higher levels of trehalose, Pro, and polyols (glycerol) than wild-type plants, which is in accordance with their enhanced tolerance to abiotic stress.

Secondary Metabolite Profile of *JUB1* Transgenics

Secondary metabolites confer various advantages to the plants, such as regulation of development and response to biotic and abiotic stresses. To study secondary metabolite profiles of *JUB1* transgenics, liquid chromatography–mass spectrometry (LC-MS) analysis was performed on extracts from rosette leaves of 35-d-old *JUB1* overexpression and *jub1-1* lines. Moreover, to identify JUB1-regulated genes involved in secondary metabolism, we tested by qRT-PCR the expression of 94 genes encoding enzymes and TFs that regulate the biosynthetic pathway from shikimate to phenylpropanoids, including anthocyanins, flavonols, and sinapoyl derivatives (see Supplemental Data Set 4 online). Our metabolite analysis revealed the most drastic changes for cyanidin derivatives (Figure 12). Cyanidin derivative (A11 and A9; Tohge et al., 2005) levels were significantly decreased in *35S*:*JUB1* plants, whereas no significant change was observed for the level of anthocyanidins in the *jub1-1* mutant. Accordingly, expression of genes encoding dihydroflavonol 4-reductase (DFR; At5g42800), a key enzyme in shunting flavonols into the anthocyanins, leucoanthocyanidin dioxygenase (LDOX; At4g22880), anthocyanin glycosyltransferases (A5GT, At4g14090; A3G2"XT, At5g54060), anthocyanin acyltransferases (A5GMaT, At3g29590; A3GCouT, At1g03940), and GST (TT19, At5g17220) were significantly downregulated in *JUB1* overexpression plants. Similarly, expression of anthocyanin regulatory

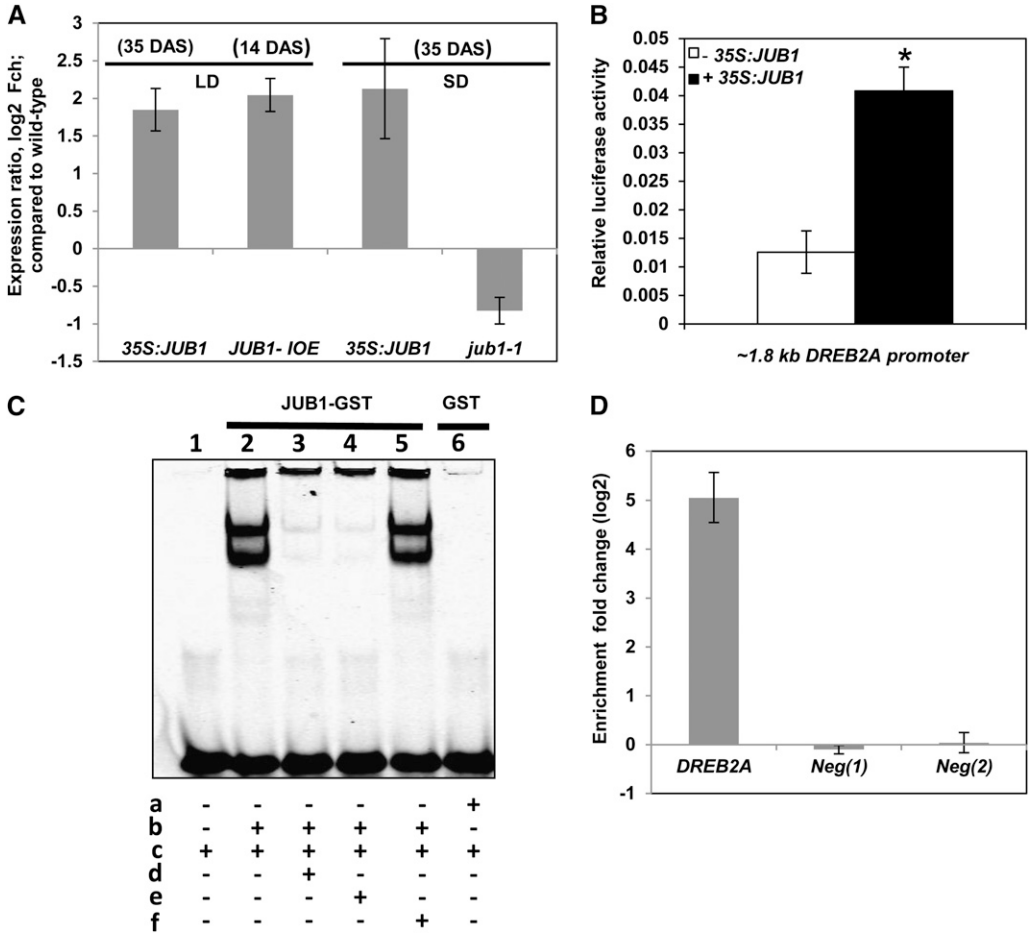

Figure 10. *DREB2A* Is a Direct Target of JUB1.

(A) Expression of *DREB2A* in *35S:JUB1*, *JUB1-IOE*, and *jub1-1* lines compared with the wild type. Plant ages are indicated in days after sowing (DAS). LD, long day; SD, short day. Numbers on the *y* axis indicate expression fold change (log2 basis) compared with the wild type. Data represent means ± SD of five (LD) or three (SD) independent experiments.

(B) Transactivation of *DREB2A* expression (from its ~1.8-kb promoter) by JUB1 in *Arabidopsis* mesophyll cell protoplasts. The Pro_{DREB2A}:*FLuc* construct harboring the *DREB2A* promoter upstream of the firefly (*Photinus pyralis*) luciferase (FLuc) open reading frame was cotransformed with the *35S:JUB1* plasmid (omitted in control experiments). The *35S:RLuc* vector was used for transformation efficiency normalization. Bars indicate the SD of at least four biological replicates. The asterisk indicates significant difference to control at $P < 0.05$.

(C) EMSA. Purified JUB1-GST protein binds specifically to the JUB1 binding site within the *DREB2A* promoter. In vitro DNA binding reactions were performed with the 40-bp wild-type fragment of the *DREB2A* promoter containing the JUB1 motif (5′-GATGCCGTTAGAGACACG-3′). a, GST protein; b, JUB1-GST protein; c, 5′-DY682 double-stranded oligonucleotide containing the perfect JUB1 binding site; d, 100× competitor (unlabeled oligonucleotide containing perfect JUB1 binding site); e, 200× competitor (unlabeled oligonucleotide containing perfect JUB1 binding site); f, 200× mutated oligonucleotide (unlabeled with mutation in JUB1 binding site where 5′-GATGCCGTTAGAGACACG-3′ was replaced by 5′-GATGCCAATA-GAGACACG-3′).

(D) ChIP-qPCR. Whole shoots of 35-d-old *Arabidopsis* plants expressing GFP-tagged JUB1 under the control of the CaMV 35S promoter (*35S:JUB1-GFP*) and wild-type plants were harvested for the ChIP experiment. qPCR was used to quantify enrichment of the *DREB2A* promoter. As negative controls, primers annealing to promoter regions of two *Arabidopsis* genes lacking a JUB1 binding site, At3g18040 (Neg 1) and At2g22180 (Neg 2), were used. Data represent means ± SD of three independent experiments.

TFs of the MYB (*PAP1* and *PAP2*), bHLH (*TT8*), and WRKY (*TTG2*) families was also reduced in *JUB1* overexpression plants compared with the wild type. Expression of *PRODUCTION OF ANTHOCYANIN PIGMENT2* (*PAP2*) was significantly induced in *jub1-1* knockdown plants (see Supplemental Figure 12 online). Apart from *PAP2*, expression of anthocyanin biosynthesis genes was either not affected or only slightly reduced in *jub1-1* knockdown plants. These data indicate that JUB1, most probably in conjunction with other TFs, negatively regulates the expression of the anthocyanin biosynthesis genes. Anthocyanins represent a group of flavonoids that accumulate under conditions of various types of environmental stresses. Moreover, they accumulate

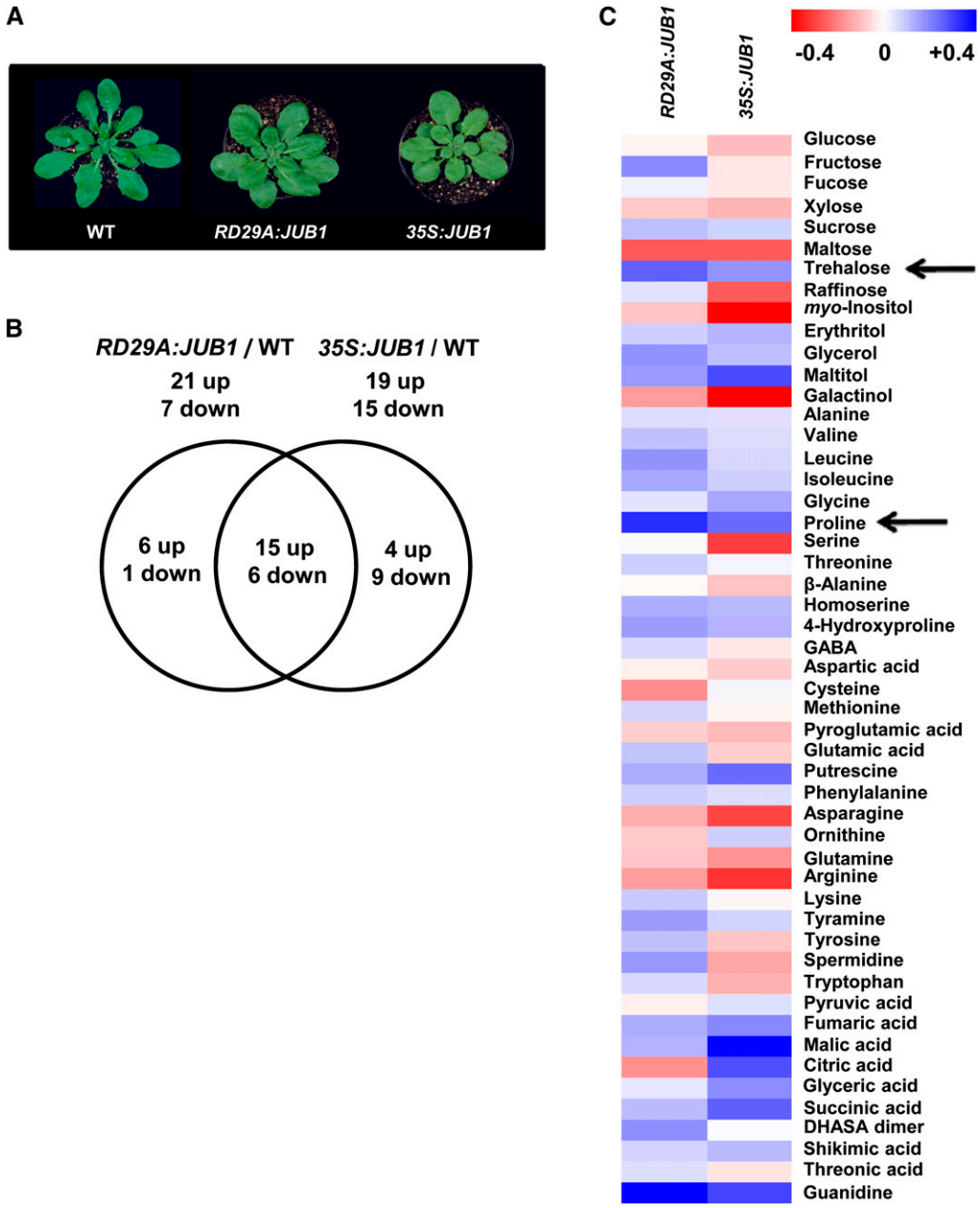

Figure 11. Primary Metabolite Profiling of *JUB1* Overexpression Plants.

(A) Phenotype of 35-d-old wild-type (WT), *RD29A*:*JUB1*, and *35S*:*JUB1* plants subjected to metabolite profiling.

(B) Venn diagram showing an overview of metabolites that are significantly different ($P < 0.05$, Student's *t* test) in *35S*:*JUB1* and *RD29A*:*JUB1* lines compared with the wild type.

(C) Hierarchical average linkage clustering of all detected primary metabolites. For every metabolite, the metabolic content of the wild type was considered as 1 and the metabolic content of overexpression lines was normalized to that. Metabolic ratios: red, minimum (between 0 and −0.4); blue, maximum (between 0 and + 0.4); see also Supplemental Data Set 3 online. Arrows indicate increased trehalose and Pro content in *JUB1* overexpressors compared with the wild type.

in senescing leaves preceding chlorophyll breakdown and play a photoprotective role against strong light in combination with coolness that may occur during autumn (Hoch et al., 2003; Diaz et al., 2006). The reduced level of anthocyanins in *JUB1* overexpression plants is consistent with their prolonged longevity.

Of the other secondary metabolites, one of the major phenylpropanoid compounds, sinapoylmalate, was significantly induced in the *JUB1* overexpression plants (Figure 12). Similarly, transcript levels of several genes encoding enzymes of phenylpropanoid metabolism, such as *FAH1* (encodes ferulate-5-hydroxylase), *ALDH* (aldehyde dehydrogenase 2C4), and *SMT* (sinapoylglucose:malate

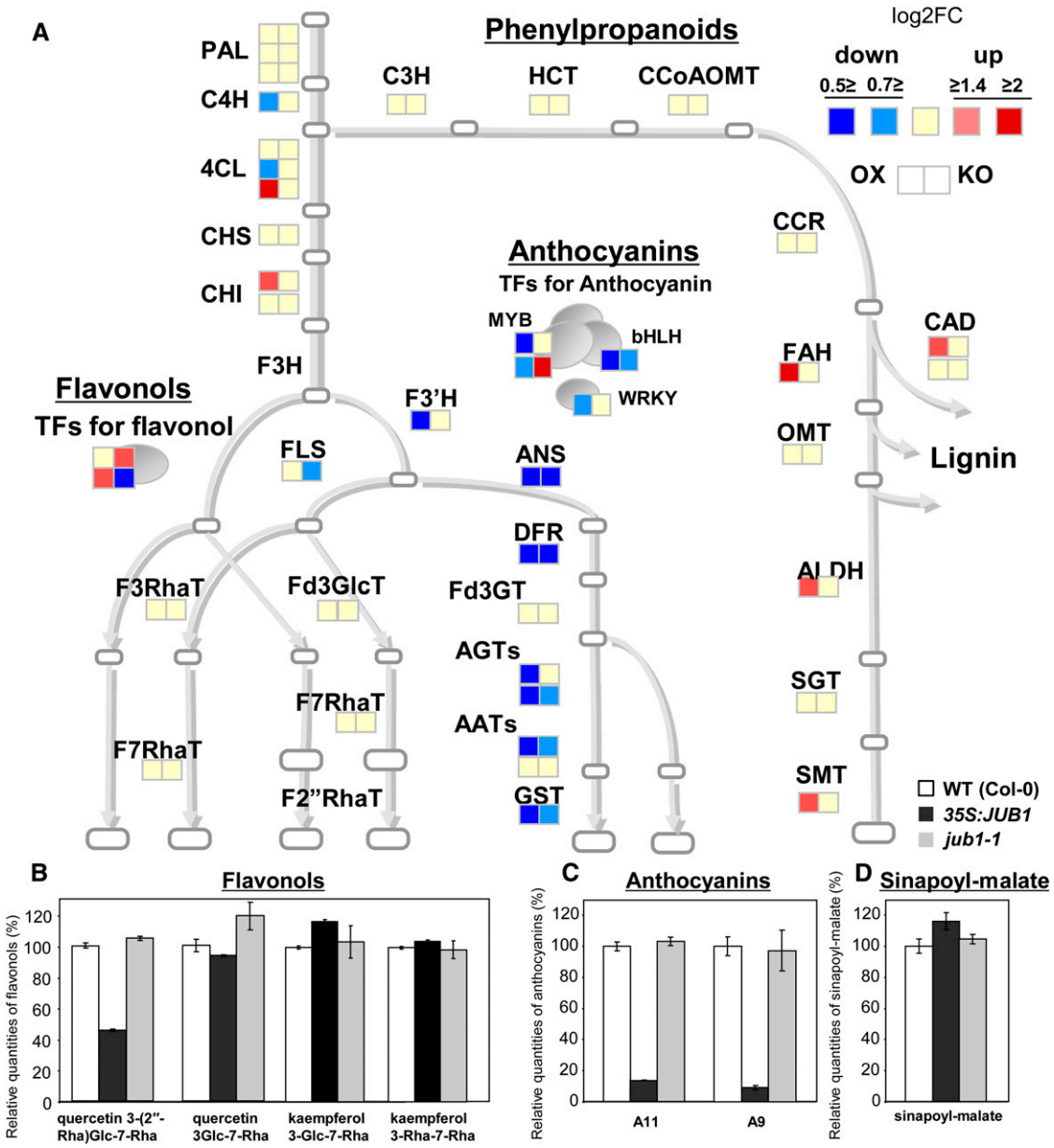

Figure 12. Gene Expression Profiling of Phenylpropanoids, Flavonols, and Anthocyanins, and Metabolite Profiling of Related Secondary Metabolites in *35S*:*JUB1*, *jub1-1*, and Wild-Type Plants.

(A) Expression of 33 enzymatic genes and six TFs as measured by qRT-PCR. Intensity of fold change against wild-type (WT) expression level ($\log_2$FC) is indicated by color. Abbreviations are given in Supplemental Table 2 online.

(B) to **(D)** The content of flavonols [quercetin-3-*O*-(2′′-*O*-Rha)Glc-7-*O*-Rha, quercetin-3-*O*-Glc-7-*O*-Rha, kaempferol-3-*O*-Glc-7-*O*-Rha, and kaempferol-3-*O*-Rha-7-*O*-Rha], anthocyanins (A11 and A9; Tohge et al., 2005), and sinapoyl-malate in *35S*:*JUB1*, *jub1-1*, and wild-type plants was analyzed by LC-MS. Average of two biological replicates ± SD.

sinapoyltransferase, which catalyzes the formation of sinapoyl-malate from sinapoylglucose), were induced in *JUB1* overexpression plants (see Supplemental Figure 12 online).

Hormonal Adjustments in *JUB1* Transgenics

Plant hormones play an important role in regulating senescence (in particular cytokinins) and the response to stress (including ABA, salicylic acid [SA], and jasmonic acid [JA]). We determined the concentrations of these hormones in rosette leaves of 43-d-old *35S*:*JUB1*, *jub1-1*, and wild-type plants. Significantly higher levels of isopentenyladenosine (IPA) and zeatin riboside (ZR) were detected in leaves of *35S*:*JUB1* transgenics compared with *jub1-1* and wild-type plants (Figure 13A), while levels of zeatin (Z), dihydrozeatin (DHZ), and dihydrozeatin riboside (DHZR) were not

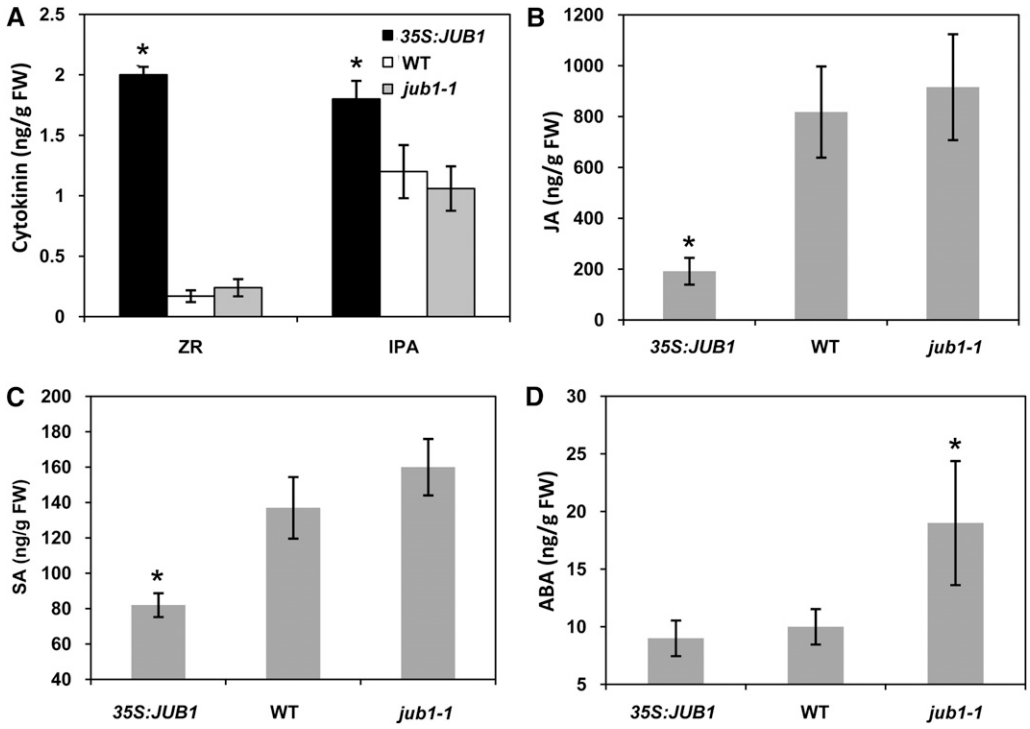

Figure 13. Hormone Contents in *35S*:*JUB1*, *jub1-1*, and Wild-Type Plants.

Determination of ZR and IPA **(A)**, JA **(B)**, SA **(C)**, and ABA **(D)** in 43-d-old *35S*:*JUB1*, *jub1-1*, and wild-type plants grown at long-day conditions (16 h light/8 h dark). Values represent the means ± SD from five independent sets of samples. Asterisks indicate significant differences compared with the wild type (WT) ($P < 0.05$, Student's *t* test). FW, fresh weight.

significantly altered (see Supplemental Figure 6C online). By contrast, levels of the biotic stress hormones JA and SA were significantly reduced in *35S*:*JUB1* lines compared with the wild type (Figures 13B and 13C), while ABA was not affected (Figure 13D). However, ABA was increased by ~94% in *jub1-1* mutant plants compared with the wild type (Figure 13D).

DISCUSSION

To identify novel regulators of plant senescence, we screened NAC overexpression and T-DNA insertion lines for changes in leaf senescence. We previously reported the identification of *ORS1* as a TF that positively regulates senescence (Balazadeh et al., 2011). Similarly, At *NAP* and *ORE1* (*ANAC092*) have been shown to act as positive regulators of senescence in *Arabidopsis* (Guo and Gan, 2006; Kim et al., 2009; Balazadeh et al., 2010a). Here, we discovered another member of the NAC gene family, designated *JUB1*, which in contrast with these previously characterized NAC factors, strongly delays senescence when overexpressed in transgenic plants and triggers precocious senescence at low expression level (in the *jub1-1* mutant and artificial microRNA lines). Thus, JUB1 represents a strong negative regulator of senescence whose molecular function may differ from those of the positively acting NAC factors. Notably, the expression of all four NACs is triggered by H_2O_2, although the H_2O_2-dependent induction is slightly less pronounced for *ORE1* compared with At *NAP*, *ORS1*, and *JUB1* (Balazadeh et al., 2010b). Additionally, the expression of several other senescence-regulated NAC genes, such as *ANAC032*, *ATAF1*, and *ANAC102*, is triggered by H_2O_2 (Balazadeh et al., 2010b). This observation is interesting and suggests a close regulatory node connecting the accumulation of cellular H_2O_2 to the regulation of senescence and possibly bolting, a developmental process often tightly linked with the onset of leaf senescence (Levey and Wingler, 2005; Balazadeh et al., 2008a). However, a distinct role during senescence has not been reported for the other NACs so far. Recently, VNI2 (*ANAC083*; At5g13180) was found to regulate senescence by integrating ABA signaling (Yang et al., 2011); it also regulates xylem vessel specification (Yamaguchi et al., 2010). Currently, however, it remains largely unknown how these diverse cellular functions are integrated by VNI2.

Similar to observations in animals, extended longevity in plants is known to be correlated with increased tolerance to oxidative stress (Finkel and Holbrook, 2000; Muller et al., 2007). The correlation between stress tolerance and the onset of senescence and determination of life span in plants is supported by experimental evidence (Jing et al., 2003). Additionally, increased stress tolerance was also observed for late-flowering/long-living *gigantea*, *ore1*, *ore3*, and *ore9* mutants (Kurepa et al., 1998; Woo et al., 2004). It has been suggested that aging is triggered by oxidative stress as a result of an imbalance between production and scavenging of oxygen radicals. In plants, this hypothesis is in part supported by the observation that timing of senescence is altered in mutants with a decreased level of the antioxidant

L-ascorbic acid (vitamin C). The *vtc1* mutant enters senescence prematurely and is more sensitive to various oxidative stresses than the corresponding wild type (Barth et al., 2004). Compared with other ROSs, H_2O_2 has a relatively long half-life of ~1 ms, although its stability is influenced by the cellular pH and redox equilibrium (Reth, 2002). H_2O_2 acts as a signaling molecule that regulates plant development and adaptation to various stresses. It has been observed that a decrease of catalase (CAT2) and cytosolic ascorbate peroxidase 1 (APX1) activities during bolting time is followed by an accumulation of H_2O_2 and an enhanced expression of the senescence-associated TF *WRKY53*, suggesting H_2O_2 functions as a signal to promote senescence (Ye et al., 2000; Miao et al., 2004; Zimmermann et al., 2006).

Although the precise molecular pathways through which JUB1 regulates longevity and abiotic stress tolerance are not known at present, one possible scenario is that it does so by affecting a gene regulatory network that possibly involves *DREB2A*, its direct downstream target. DREB2A is an important transcription regulator acting in response to various abiotic stresses (e.g., Sakuma et al., 2006a; Kant et al., 2008). Transcriptome studies have shown that DREB2A activates a large number of abiotic stress–responsive genes involved in drought and heat stress responses (Sakuma et al., 2006b). The heat shock TF gene *HsfA3* has been identified as a direct downstream target of DREB2A during heat stress (Schramm et al., 2008; Yoshida et al., 2008), and *DREB2A* itself is a heat shock–responsive gene (Suzuki et al., 2011). Another direct target of DREB2A is *RESPONSIVE TO DESSICATION29A* (*RD29A*; also referred to as *COR78*; Liu et al., 1998). Although we have not experimentally tested heat stress–dependent *JUB1* expression here, global transcriptome data from Swindell (2006) identified *JUB1* as a heat stress–responsive gene. Another observation of interest is that all three genes are significantly upregulated by H_2O_2 treatment (10 mM, 5 h) in *Arabidopsis* seedlings, although induction levels varied between the three TF genes (*JUB1*, ~25-fold; *DREB2A*, ~90-fold; *HsfA3*, approximately threefold; see Supplemental Figure 6D online). Taken together, our data in conjunction with published reports (Schramm et al., 2008; Yoshida et al., 2008) establish an extended transcriptional cascade involving three consecutive positive regulators (JUB1–DREB2A–HsfA3), with JUB1 adopting an upstream position. Furthermore, HsfA3 has been suggested to be part of an expression amplification loop (Nishizawa-Yokoi et al., 2011) involving two additional heat shock TFs (i.e., HsfA1e and HsfA2), where HsfA1e activates *HsfA2* expression (likely by direct binding to heat shock *cis*-elements present in its promoter; Nishizawa-Yokoi et al., 2011), HsfA2 activates *HsfA3* expression (Schramm et al., 2006), and HsfA3 stimulates expression of *HsfA1e* (Yoshida et al., 2008). HsfA2 has been shown to directly regulate the expression of *APX2*, which encodes a key cytosolic enzyme for the detoxification of H_2O_2 (Shigeoka et al., 2002; Nishizawa et al., 2006; Schramm et al., 2006), consistent with our observation of reduced H_2O_2 level in *JUB1* overexpressors. The control network linking H_2O_2 signaling with this Hsf activation loop most likely involves additional transcriptional regulators, including MBF1c, which was shown to be required for enhanced expression of *DREB2A* during heat stress (Suzuki et al., 2011). Notably, *MBF1c* is highly responsive to abiotic stresses, including heat stress (Suzuki et al., 2011), and is also rapidly and strongly upregulated by H_2O_2 treatment (~30-fold up already after 1 h at 10 mM H_2O_2; see Supplemental Figure 6E online). As we have shown here (Table 1), MBF1c is significantly more upregulated after H_2O_2 challenge in *JUB1* overexpressors than in the *jub1-1* mutant, further supporting the model of a regulatory link between JUB1 and MBF1c upstream of *DREB2A* and *HsfA3*. In accordance with this model is the observation that *MBF1c* contains a JUB1 binding site (CGCCGT) in its promoter at around 640 bp upstream of the transcription start site; however, we have not yet tested its functional relevance.

Our analysis presented here also identified changes in primary and secondary metabolism in *JUB1* transgenic lines. In general, our analysis revealed an accumulation of various compatible solutes, including trehalose, Pro, and various sugar alcohols (maltitol, glycerol, and erythritol) in *JUB1* overexpressors compared with wild-type plants, which may contribute to the enhanced abiotic stress tolerance of such lines. Although the role of these metabolites in senescence is not well established, examples indicate that trehalose and sugar alcohols (mannitol and inositol) delay senescence of cut flowers in some species (reviewed in van Doorn and Woltering, 2008). We also noticed a significant increase

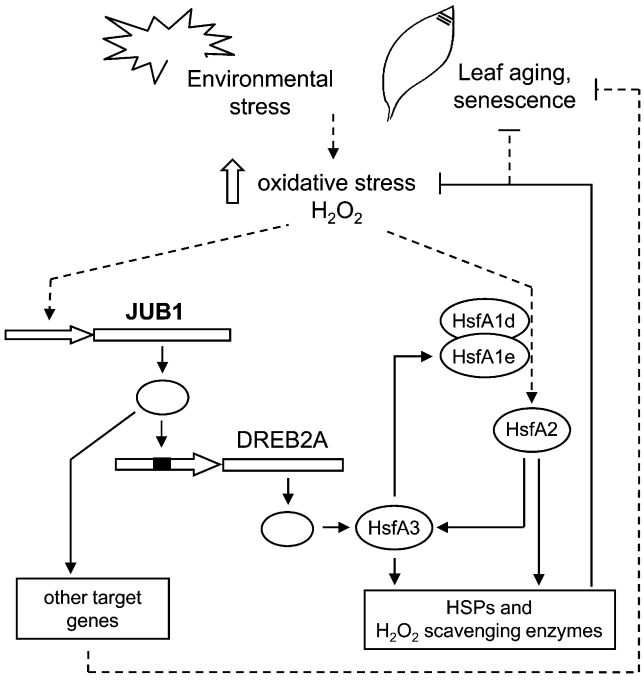

Figure 14. Model of JUB1 Action.

JUB1 is activated by H_2O_2 and during leaf senescence. JUB1 TF binds to the *DREB2A* promoter, thereby activating its expression. DREB2A positively regulates the expression of *HsfA3* (Schramm et al., 2008; Yoshida et al., 2008), thus establishing a transcriptional cascade. As suggested by Nishizawa-Yokoi et al. (2011), HsfA3 together with Hsf1A1e and HsfA2 form an expression amplification loop. HsfA3 and HsfA2 regulate the expression of *HSPs* and H_2O_2 scavenging enzymes, leading to reduced intracellular H_2O_2 levels, extended longevity, and increased stress tolerance. Increased longevity may also be regulated through other JUB1 target genes.

in Suc concentration due to *JUB1* overexpression. At the level of secondary metabolites, we observed a decrease of cyanidin derivatives upon *JUB1* overexpression, which was accompanied by reduced expression of anthocyanin biosynthesis genes (including *DFR*, *LDOX*, *A5GT*, and others) and known anthocyanin regulatory TFs (i.e., *PAP1*, *PAP2*, *TTS*, and *TTG2*). By contrast, expression of *PAP2* was significantly induced in *jub1-1* knockdown plants. Our data thus indicate that JUB1, possibly jointly with other TFs, has a negative effect on the expression of anthocyanin biosynthesis genes. Anthocyanins accumulate as a response to various types of environmental stresses and in senescing leaves, where they play a photoprotective role against high light stress in combination with low temperature, which occurs, for instance, in autumn (Hoch et al., 2003; Diaz et al., 2006). The reduced anthocyanin level in *JUB1* overexpression plants is consistent with their prolonged longevity. Furthermore, minor flavonol glycosides, such as quercetin glycosides, were slightly decreased in leaves of *JUB1* overexpressors. This may be due to the downregulated expression of F3′H (*TT7*) caused by the suppression of *PAP1*. Despite this fact, the increased levels of other effective phenolic antioxidants, like sinapoyl-malate and major glycosides of kaempferol, may contribute to the enhanced oxidative stress tolerance (Figure 12).

At the hormone level, we found higher levels of cytokinins (ZR and IPA) in *JUB1* overexpressors. Cytokinins are important regulators of senescence, and leaf senescence and the induction of SAGs can only be initiated when cytokinin levels are below a threshold (Gan and Amasino, 1995; Noodén et al., 1997). The high cytokinin level in *JUB1* overexpressors is thus in accordance with their extended lifespan. On the contrary, ABA level increased in the *jub1-1* mutant, indicating cellular stress, possibly due to disturbed H_2O_2 homeostasis in these plants.

Model for JUB1 Action

Based on the available experimental data, we propose the following model for JUB1 action (Figure 14). *JUB1* transcription is activated by a rise of endogenous H_2O_2 concentration that is triggered by developmental input or environmental stress, including wounding, salinity stress, or cellulase treatment. Notably, *JUB1* expression follows the cellular H_2O_2 concentration that changes with plant development, showing a peak during bolting (Zimmermann et al., 2006). The upstream TF(s) regulating H_2O_2-dependent or senescence-associated *JUB1* transcription remains unknown at present. JUB1 directly targets *DREB2A*, which functions as a positive regulator of *HsfA3* and *RD29A*. HsfA3 itself regulates the expression of *HSP* genes and is part of a positive feedback loop together with HsfA1e and HsfA2 (Nishizawa-Yokoi et al., 2011), whereas the molecular function of RD29A is not known. Elevation of *JUB1* expression lowers H_2O_2 concentration in plant tissues, possibly through the Hsf amplification loop, while the opposite effect (i.e., increased H_2O_2 concentration) is observed in the *jub1-1* mutant, suggesting that JUB1 assists in regulating cellular H_2O_2 homeostasis. Although the precise molecular mechanism through which JUB1 regulates intracellular H_2O_2 concentration remains to be established, the current model proposes an involvement of HSPs and H_2O_2 scavenging enzymes. Notably, several GST genes (including *GST10*, *24*, and *25*) were induced in *JUB1* overexpressors after H_2O_2 treatment, while expression of these genes remained either unchanged or was slightly reduced in the *jub1-1* mutant (Table 1).

Concomitant with enhanced *JUB1* expression, we observed reduced expression of many SAGs, which is in accordance with the delayed senescence observed in these lines. Notably, expression of SAGs is increased in the *jub1-1* mutant, constituting JUB1 as a negative regulator of senescence. A possible explanation of the reduced expression of SAGs in *JUB1* overexpressors may be derived from the observation that expression of many SAGs is enhanced by H_2O_2 (e.g., Navabpour et al., 2003; Balazadeh et al., 2010b; Genevestigator at http://www.genevestigator.com). In particular, expression of the majority of the senescence-associated NAC TFs is also triggered by H_2O_2 treatment (15 NACs in total), including At *NAP*, *ORS1*, and *ORE1* (Balazadeh et al., 2010b), all of which have been shown to affect senescence positively. Thus, our model suggests that JUB1 lowers the cellular H_2O_2 level, thereby minimizing the stimulatory effect on NAC gene expression and, hence, senescence. On the contrary, reduced *JUB1* expression (such as in the *jub1-1* mutant) would favor the accumulation of cellular H_2O_2 that drives NAC gene expression and through this supports precocious senescence. However, there is also the additional possibility that JUB1 regulates senescence through other target genes of currently unknown molecular function (Figure 14). Future work will have to address the intricacies of the underlying regulatory network in greater detail.

METHODS

General

Standard molecular techniques were performed as described (Sambrook et al., 2001; Skirycz et al., 2006). Oligonucleotide sequences are given in Supplemental Data Set 5 online. Chemicals and reagents for GC-MS analysis were obtained from Sigma-Aldrich, Fluka, or Merck with the exception of *N*-methyl-*N*-(trimethylsilyl) trifluoroacetamide, which was obtained from Macherey-Nagel. For sequence analyses, the tools provided by the National Center for Biotechnology Information (http://www.ncbi.nlm.nih.gov/), MIPS (http://mips.gsf.de/), The Arabidopsis Information Resource (http://www.arabidopsis.org/), and the Plant Transcription Factor Database (http://plntfdb.bio.uni-potsdam.de/v3.0/) were used.

Plants

Seeds of *Arabidopsis thaliana* accession Col-0 were obtained from the *Arabidopsis thaliana* Resource Centre for Genomics (Institut National de la Recherche Agronomique, France; http://dbsgap.versailles.inra.fr/publiclines/). For growth under long-day conditions, seedlings were grown in soil (Einheitserde GS90; Gebrüder Patzer) in a climate-controlled chamber with a 16-h daylength provided by fluorescent light at ~100 μmol m^{-2} s^{-1} and a day/night temperature of 20/16°C and a RH of 60/75%. After 2 weeks, seedlings were transferred to a growth chamber with a 16-h day (80 or 120 μmol m^{-2} s^{-1}) and a day/night temperature of 22/16°C and 60/75% RH. For growth under short-day conditions, the light period was reduced to 8 h. Growth in hydroponic culture, salinity treatment, and sample preparation were done as described using stage 1 plants (28 d old) (Balazadeh et al., 2010a). T-DNA insertion lines screened for extended longevity (see Supplemental Table 1 online) were obtained from the European Arabidopsis Stock Centre (http://Arabidopsis.info/). Homozygous plants were identified by PCR using the T-DNA left border primer, as well as the gene-specific primers LP and RP.

Constructs

Constructs were generated by PCR- and restriction enzyme-mediated cloning. Primer sequences are given in Supplemental Data Set 5 online. PCR-generated amplicons were checked by DNA sequence analysis (MWG). Constructs were transformed into *Arabidopsis* Col-0 via *Agrobacterium tumefaciens*–mediated transformation.

For *35S*:*JUB1*, the *JUB1* open reading frame was amplified by PCR from *Arabidopsis* Col-0 leaf cDNA and inserted into pUni/V5-His-TOPO (Invitrogen). The cDNA was cloned via added *Pme*I-*Pac*I sites into a modified pGreen0229-35S plant transformation vector (Skirycz et al., 2006). For *RD29A*:*JUB1*, the *RD29A* promoter (1 kb upstream of translation start site) was amplified from *Arabidopsis* (Col-0) genomic DNA, cloned into pCR2.1 (Invitrogen), and then transferred via *Bam*HI and *Nco*I sites into pCAMBIA1305.1-hygromycin, giving rise to plasmid RD29A:pCAMBIA. The *JUB1* coding region was amplified by PCR from leaf cDNA using primers JUB1-forward and JUB1-reverse and cloned downstream of the *RD29A* promoter in plasmid RD29A:pCAMBIA via primer-added *Nco*I and *Pml*I sites. For *35S*:*JUB1-GFP*, the full-length *JUB1* open reading frame was amplified without its stop codon. The PCR product was cloned into the pENTR/D-TOPO vector using the pENTR Directional TOPO cloning kit (Invitrogen). The sequence-verified entry clone was then transferred to the pK7FWG2 vector (Ghent University) by LR recombination (Invitrogen). For *JUB1-IOE*, the *JUB1* coding region was amplified by PCR from *Arabidopsis* leaf cDNA using primers JUB1-IOE-fwd and JUB1-IOE-rev, inserted into pBluescript SK$^+$, and then cloned via *Xho*I and *Spe*I sites into the pER8 vector (Zuo et al., 2000). For the Pro_{JUB1}:*GUS* fusion, an ~1.8-kb 5′ genomic fragment upstream of the translation initiation codon was amplified by PCR from *Arabidopsis* Col-0 genomic DNA, inserted into plasmid pGEM-T Easy (Promega), and fused via *Hin*dIII (present in pGEM-T Easy) and *Nco*I restriction sites to the *GUS* reporter gene in pCAMBIA1305.1-hygromycin (CAMBIA). For *JUB1-amiRNA*, the Web MicroRNA Designer platform (http://wmd2.weigelworld.org/cgi-bin/mirnatools.pl?page=1) was used to design amiRNA sequences (21-mers). For Pro_{DREB2A}:*FLuc*, the ~1.8-kb *DREB2A* promoter containing the JUB1 binding site was amplified by PCR from *Arabidopsis* genomic DNA and inserted into the pENTR/D-TOPO vector (Invitrogen). The sequence-verified promoter was then transferred to the p2GWL7.0 vector harboring the firefly (*Photinus pyralis*) luciferase (FLuc) coding region (Licausi et al., 2011) by LR recombination (Invitrogen).

Expression Profiling by qRT-PCR

Total RNA extraction, synthesis of cDNA, and qRT-PCR were performed as described (Caldana et al., 2007; Balazadeh et al., 2008b). Expression analysis platforms contained primer pairs for 168 SAGs (Parlitz et al., 2011), 179 ROS-responsive genes, and 94 phenolic secondary metabolite biosynthetic genes. Genes included in the SAG platform are highly upregulated during natural senescence in wild-type *Arabidopsis* plants (Buchanan-Wollaston et al., 2005; van der Graaff et al., 2006; Balazadeh et al., 2008b). ROS-responsive genes were extracted from the literature (Gechev et al., 2004, 2005; Davletova et al., 2005a, 2005b; Gadjev et al., 2006) and in-house experiments. Primers for the metabolite platform were designed for the biosynthetic genes from primary metabolism to flavonoid production; the platform also included primers for other phenolic secondary metabolite biosynthetic genes and TFs that control anthocyanin biosynthesis. Genes included in the qRT-PCR platforms, including primer sequences, are given in Supplemental Data Set 5 online. Primers were designed using QuantPrime (Arvidsson et al., 2008). PCR reactions were run on an ABI PRISM 7900HT sequence detection system (Applied Biosystems Applera), and amplification products were visualized using SYBR Green (Applied Biosystems). *ACTIN2* served as reference gene; primers were Actin2-F (5′-TCCCTCAGCACATTCCAGCAGAT-3′) and Actin2-R (5′-AACGATTCCTGGACCTGCCTCATC-3′).

DNA Binding Site Selection

In vitro binding site selection was performed using the CELD system with the pTacJUB1-LCELD6XHis construct, employing three biotin-labeled double-stranded oligonucleotides (i.e., Bio-RS-Oligo 1, RS-Oligo 2, and Bio-RS-Oligo 3), which contained 30-nucleotide random sequences that differed in flanking primer sequence (Xue, 2005). JUB1-selected oligonucleotides were cloned and sequenced. The DNA binding activity of JUB1-CELD was measured using methylumbelliferyl β-D-cellobioside as substrate (Xue, 2002). DNA binding assays with a biotin-labeled single-stranded oligonucleotide or a biotin-labeled double-stranded oligonucleotide without a target binding site were used as controls.

Transactivation Assays

Arabidopsis mesophyll cell protoplasts were prepared according to the protocol of Sheen (2002). The construct containing the ~1.8-kb *DREB2A* promoter fragment in front of the FLuc coding region (Pro_{DREB2A}:*FLuc*) was cotransformed in the presence or absence of the *35S*:*JUB1* plasmid. The *35S*:*RLuc* vector (Licausi et al., 2011) was used for normalization against transformation efficiency. Firefly luciferase and *Renilla* luciferase (RLuc) were assayed using the Dual Luciferase Reporter Assay System (Promega). Six micrograms of DNA were used for transient transformation of protoplasts according to Yoo et al. (2007); 16 h after incubation, protoplasts were lysed by adding 400 μL of passive lysis buffer, and the resulting suspension was briefly vortexed. Forty microliters of luciferase assay buffer was added to the same volume of crude extract and FLuc activity was measured. Forty microliters of Stop and Glow buffer was then added and *Renilla* chemiluminescence was measured. Relative light units were determined in a GloMax 20/20 luminometer (Promega) using a 10-s measurement. Data were collected as ratio (FLuc activity:RLuc activity). Protoplasts transformed with only the promoter-FLuc, *35S*:*RLuc* reporter plasmid (no TF), were analyzed as background controls.

EMSA

JUB1-GST fusion protein was purified from *Escherichia coli* expression strain BL21 Star (DE3) pRARE, which was generated by transforming the pRARE plasmid isolated from Rosetta (DE3) pRARE cells (Merck) into *E. coli* BL21 Star (DE3) (Invitrogen). Protein expression was induced in a 100-mL expression culture using 1 mM isopropyl thio-β-D-galactoside, and cells were harvested 4 h after induction at 30°C. Cells were sonicated in lysis buffer (20 mM sodium phosphate buffer, pH 7.3, 150 mM NaCl, 1 mM EDTA, 1 mM DTT, and 1 mM phenylmethanesulfonyl fluoride). Supernatant of centrifuged sample was used for purification using a 1-mL GSTrap HP column (GE Healthcare) coupled to the Äkta-Purifier FPLC system (GE Healthcare). Aliquots of the flow-through fractions were analyzed by SDS-PAGE and Coomassie Brilliant Blue staining. One-milliliter elution fractions containing the purified JUB1-GST fusion protein were pooled and dialyzed against PBS buffer (20 mM Na-phosphate, pH 7.4, and 150 mM NaCl). Protein concentration was determined by the Bradford assay (Bradford, 1976). 5′-DY682-labeled DNA fragments were ordered from MWG. Sequences of labeled DNA fragments, unlabeled competitors, and mutated fragments are given in Supplemental Data Set 5 online. Annealing was performed by heating the primers to 100°C followed by slow cooling to room temperature. The binding reaction was performed at room temperature for 20 min as described in the Odyssey Infrared EMSA kit instruction manual. DNA-protein complexes were separated on 6% retardation gel, while DY682 signal was detected using the Odyssey Infrared Imaging System from LI-COR Biosciences.

In Vivo Binding of JUB1 to the *DREB2A* Promoter

To investigate in vivo binding of JUB1 to its DNA binding site in the *DREB2A* promoter, we used ChIP-qPCR, using whole shoots from long day–grown,

35-d-old *Arabidopsis* plants expressing GFP-tagged JUB1 protein from the CaMV 35S promoter (*35S:JUB1-GFP*). Wild-type plants were used as negative control. For the ChIP, we followed a protocol previously described by Kaufmann et al. (2010) employing anti-GFP antibody to immunoprecipitate protein-DNA complexes. The ChIP experiment was run in three independent replications. qPCR was used to test binding of JUB1 to its binding site within the *DREB2A* promoter; the primers flanked the JUB1 binding site. As a negative control, we used primers annealing to promoter regions of two other *Arabidopsis* genes (At3g18040 and At2g22180) lacking a JUB1 binding site. Primer sequences are given in Supplemental Data Set 5 online. We analyzed ChIP-qPCR data relative to input, as this includes normalization for both background levels and input chromatin going into the ChIP. The amount of genomic DNA coprecipitated by GFP antibody (ChIP signal) was calculated in comparison to the total input DNA used for each immunoprecipitation in the following way: cycle threshold (C_T) = C_T(ChIP) − C_T(Input). To calculate fold enrichment, normalized ChIP signals were compared between *35S:JUB1-GFP* and wild-type plants, where the ChIP signal is given as the fold increase in signal relative to the background signal.

H_2O_2 Measurements

The H_2O_2 staining agent, DAB (D5637, Sigma-Aldrich), was dissolved in water and adjusted to pH 3.8 with KOH. To avoid auto-oxidation, the DAB solution was freshly prepared (Fryer et al., 2002). Whole seedlings were infiltrated under vacuum with 0.5 mg mL^{-1} DAB staining solution and further incubated for 12 h in medium; chlorophyll was removed by incubating seedlings in 90% ethanol at 70°C for 10 min. H_2O_2 was visualized as brown color due to DAB polymerization.

Quantitative measurement of H_2O_2 production was performed using the Amplex Red hydrogen peroxide/peroxidase assay kit (Molecular Probes) following the manufacturer's instructions. Briefly, samples were ground in liquid nitrogen, and 30 mg of ground frozen tissue from each sample was placed in an Eppendorf tube and kept frozen. Four hundred milliliters of 20 mM sodium phosphate buffer, pH 6.5, was immediately added into the tube and mixed. The extraction was centrifuged at 10,000*g* for 10 min at 4°C, and the supernatant was used for the assay. Measurements were performed at excitation and emission wavelengths of 560 and 590 nm, respectively, using a 96-well LS55 luminescence spectrometer (PerkinElmer). H_2O_2 levels are given in pmol/mg frozen tissue.

Primary Metabolite Profiling by GC-MS

To perform this study, we grew all plants alongside each other under carefully controlled conditions. Metabolite extraction, derivatization, and relative metabolite levels were determined using an established GC-MS protocol as described previously (Roessner et al., 2001; Lisec et al., 2006). Metabolites were identified in comparison to database entries of authentic standards (Kopka et al., 2005; Schauer et al., 2005).

Secondary Metabolite Profiling by LC-MS

Secondary metabolite analysis by LC-MS was performed as described by Tohge and Fernie (2010). All data were processed using Xcalibur 2.1 software (Thermo Fisher Scientific). The obtained data matrix was normalized using an internal standard (Isovitexin; CAS 29702-25-8). Metabolites were identified and annotated based on comparisons with data in our previous publications (Tohge et al., 2005, 2007; Hirai et al., 2007; Yonekura-Sakakibara et al., 2008), metabolite databases (reviewed in Tohge and Fernie, 2009), and standard compounds (Yonekura-Sakakibara et al., 2008; Nakabayashi et al., 2009).

Hormone Analyses

The extraction and analysis of ABA, SA, JA, and the cytokinins Z, ZR, DHZ, DHZR, and IPA were performed as described previously (Abreu and Munné-Bosch, 2009), except that internal deuterated standards and ultraperformance liquid chromatography–MS/MS (instead of HPLC-MS/MS) were used for the analysis. Briefly, 100 mg of leaf samples was ground in liquid nitrogen and extracted with 1.5 mL methanol using sonication. After centrifugation, the supernatant was collected and the pellet was reextracted with isopropanol:glacial acetic acid (99:1) to fully extract cytokinins. The two supernatants were dried completely under a nitrogen stream and redissolved in 150 μL methanol. Then, supernatants were combined, filtered through a 0.22-μm polytetrafluoroethylene filter (Waters), and injected into the LC-MS/MS system. MS/MS analyses were performed on an API 3000 triple quadrupole mass spectrometer (PE Sciex). All analyses were performed using the Turbo Ion Spray source in negative ion mode for ABA, SA, and JA and in positive ion mode for cytokinins. Internal standards (deuterium-labeled hormone analogs, including d_4-SA, d_6-ABA, d_5-JA, d_6-IPA, d_5-Z, and d_5-ZR purchased from OlChemIm) were added to each sample immediately after grinding, thus allowing the calculation of specific recovery rates for each compound. Quantification by MS/MS using the Multiple Reaction Monitoring method was performed as described by Abreu and Munné-Bosch (2009). Multiple Reaction Monitoring acquisition was done monitoring the following transitions: ABA, 263/153; SA, 137/93; JA, 209/59; IPA, 336/204; Z, 220/136; ZR, 352/220; DHZ, 222/136; DHZR, 354/222.2; d_6-ABA, 269/159; d_4-SA, 141/97.2; d_5-JA, 241/64; d_6-IPA, 342/210; d_5-Z, 225/137; and d_5-ZR, 357/225. The declustering potential and collision energy were optimized for each compound.

Treatments

For EST induction, 12-d-old seedlings were incubated in liquid MS medium containing 15 μM EST (control treatment: 0.15% ethanol). The seedlings were kept on a rotary shaker for 30 min or 2, 6, or 24 h, harvested, and, after removal of the roots, immediately frozen in liquid nitrogen. *JUB1* expression level was determined by qRT-PCR. For EST induction on plates, MS medium was supplemented with 10 μM EST (control: 0.1% ethanol). Cellulase treatment was performed as described (Rentel et al., 2004). Briefly, 12-d-old Col-0 seedlings grown on agar plates were transferred to liquid medium supplied with 0.1% cellulase R-10 (Onozuka R-10; Yakult). Seedlings were incubated for 5 h on a rotary shaker at continuous light, and expression of *JUB1* was determined by qRT-PCR. For histochemical GUS assays, Pro_{JUB1}:*GUS* seedlings were treated with 0.5% cellulase R-10 for 3 h. For methyl viologen (MV) treatment, 12 d-old Col-0 seedlings grown on agar plates were transferred to liquid medium, supplied with 10 μM MV (Sigma-Aldrich). Seedlings were incubated for 5 h on a rotary shaker, and expression of *JUB1* was determined by qRT-PCR. For histochemical GUS assays, Pro_{JUB1}:*GUS* seedlings were treated with 50 μM MV for 3 h. For salt treatment, seedlings grown on MS medium were transferred to liquid MS medium containing 150 or 200 mM NaCl, followed by incubation for the indicated times; alternatively, seeds were sown on MS medium containing 100 mM NaCl.

Microscopy

Distribution of JUB1-GFP fusion protein was analyzed by confocal fluorescence microscopy using an Eclipse E600 microscope (Nikon).

Other Methods

Histochemical GUS assays was performed as described by Plesch et al. (2001). Fluorometric determination of GUS activity was done using 4-MUG (Sigma-Aldrich) as substrate (Jefferson et al., 1987). Chlorophyll content was determined using a SPAD analyzer (N-tester; Hydro Agri). Alternatively, frozen *Arabidopsis* leaves were ground in liquid nitrogen, resuspended in 1 mL of 96% (v/v) ethanol, and homogenized for 1 min.

The soluble fraction, which contains chlorophyll, was separated by centrifugation (5 min, 13,000 rpm), and the amount of chlorophyll in the extract was determined spectrophotometrically at 650 nm. Ion leakage in the first six leaves was determined as described (Guo and Gan, 2006).

Statistical Analyses

Unless otherwise specified, statistical analyses were performed using Student's *t* test embedded in Microsoft Excel. Only the return of $P < 0.05$ was designated as statistically significant.

Accession Numbers

Sequence data from this article can be found in the Arabidopsis Genome Initiative or GenBank/EMBL databases under the following accession numbers: *ACTIN2* (At3g18780), *ALDH* (At3g24503), At *NAP* (At1g69490), *DREB2A* (At5g05410), *FAH1* (At4g36220), *JUB1* (At2g43000), *MBF1c* (At3g24500), *ORE1* (At5g39610), *ORS1* (At3g29035), *SMT* (At2g22990), *TT7* (At5g07990), and *VNI2* (At5g13180). Additional accession numbers are given in Supplemental Tables 1 and 2 online and Supplemental Data Sets 1, 2, 4, and 5 online.

Supplemental Data

The following materials are available in the online version of this article.

Supplemental Figure 1. Early Leaf Senescence in *JUB1-amiRNA* Lines.

Supplemental Figure 2. Localization of JUB1-GFP Fusion Protein in Guard Cells of Transgenic *Arabidopsis*.

Supplemental Figure 3. Phenotypic and Physiological Analyses of Transgenic Plants Overexpressing *JUB1* under Control of Stress-Inducible Promoter *RD29A*.

Supplemental Figure 4. Confirmation of T-DNA Insertion in *jub1-1 M*utant.

Supplemental Figure 5. Dark-Induced Senescence Is Affected in Detached Leaves of *JUB1* Overexpressors.

Supplemental Figure 6. Gene Expression and Hormone Levels in *Arabidopsis* Plants Subjected to Different Treatments.

Supplemental Figure 7. H_2O_2 Content and *JUB1* Expression Level in Individual Leaves of 35-d-Old Wild-Type Plants.

Supplemental Figure 8. Effect of NaCl, Cellulase, and Methyl Viologen on *JUB1* Expression.

Supplemental Figure 9. Effect of H_2O_2 on Detached Leaves of the *jub1-1* Mutant.

Supplemental Figure 10. The *jub1-1* Mutant Exhibits Decreased Heat Stress Tolerance Compared with the Wild Type.

Supplemental Figure 11. Enhanced Heat Stress Tolerance of *JUB1* Overexpressor.

Supplemental Figure 12. Expression of Secondary Metabolite-Associated Genes in *35S*:*JUB1*, *jub1-1*, and Wild-Type Plants, Determined by qRT-PCR.

Supplemental Table 1. NAC Transcription Factor T-DNA Insertion Lines Included in the Screen for Extended Longevity.

Supplemental Table 2. Abbreviations of Enzyme Names.

Supplemental Data Set 1. Expression of 168 Senescence-Associated Genes in 47-d-Old *35S*:*JUB1*, *jub1-1*, and Wild-Type Plants.

Supplemental Data Set 2. Expression of 179 ROS Genes in 2-Week-Old, H_2O_2-Treated (10 mM, 6 h) and Nontreated *RD29A*:*JUB1*, *jub1-1*, and Wild-type Plants.

Supplemental Data Set 3. Metabolite Composition of Rosette Leaves of 35-d-Old Wild-type, *35S*:*JUB1*, and *RD29A*:*JUB1* Plants.

Supplemental Data Set 4. Expression of 94 Secondary Metabolite-Associated Genes in 35-d-Old *35S*:*JUB1*, *jub1-1*, and Wild-Type Plants.

Supplemental Data Set 5. Oligonucleotide Sequences.

ACKNOWLEDGMENTS

B.M.-R. thanks the Deutsche Forschungsgemeinschaft (FOR 948; MU 1199/14-1) for funding and the Bundeministerium für Bildung und Forschung for funding the *Go*FORSYS Research Unit for Systems Biology (FKZ 0313924). A.W. was supported by the Chinese Academy of Sciences as a member of the Joint Doctoral Promotion Program and the National Basic Research Program of China (2009CB118604). We thank the Pakistan Higher Education Commission and the Deutscher Akademischer Austauschdienst for providing a scholarship to H.S. (DAAD A/02/37115). Prashanth Garapati is supported by funds from the International Max-Planck Research School of the Max-Planck Society and the University of Potsdam. S.M.-B. was supported by the Institució Catalana de Recerca i Estudis Avançats Academia prize funded by the Generalitat de Catalunya and the BFU2009-07294 grant funded by the Ministry of Science and Innovation of the Spanish Government. We also thank Sara Shahnejat for performing some of the heat stress experiments, Josef Bergstein for photographic work, Karin Koehl and the Green Team for expert plant care, Eugenia Maximova for help with microscopy, Isabell Witt for great support during the initiation of the project, Maren Müller for hormone analyses, and Tsanko Gechev for assistance in selecting genes for the ROS qRT-PCR expression profiling platform. We thank the European Arabidopsis Stock Centre for providing seeds of T-DNA insertion lines.

AUTHOR CONTRIBUTIONS

B.M.-R. and S.B. designed the research and supervised the group. A.D.A., A.W., H.S., P.G., and S.B. performed the research. M.-I.Z. generated the *35S*:*JUB1* lines. H.D. produced recombinant JUB1-GST protein. M.A.A.-F. and S.M.-B. performed the hormone analysis. C.A., T.T., and A.R.F. did the metabolite profiling. G.-P.X. performed the CELD experiment. K.K. and S.B. performed the ChIP experiment. B.M.-R. and S.B. wrote the article with contributions from the other authors.

Received August 31, 2011; revised December 1, 2011; accepted January 25, 2012; published February 17, 2012.

REFERENCES

Abreu, M.E., and Munné-Bosch, S. (2009). Salicylic acid deficiency in *NahG* transgenic lines and *sid2* mutants increases seed yield in the annual plant *Arabidopsis thaliana*. J. Exp. Bot. **60:** 1261–1271.

Andersson, A., et al. (2004). A transcriptional timetable of autumn senescence. Genome Biol. **5:** R24.

Arvidsson, S., Kwasniewski, M., Riaño-Pachón, D.M., and Mueller-Roeber, B. (2008). QuantPrime—A flexible tool for reliable high-throughput primer design for quantitative PCR. BMC Bioinformatics **9:** 465.

Balazadeh, S., Kwasniewski, M., Caldana, C., Mehrnia, M., Zanor, M.I., Xue, G.P., and Mueller-Roeber, B. (2011). ORS1, an H_2O_2-responsive

NAC transcription factor, controls senescence in *Arabidopsis thaliana*. Mol. Plant **4:** 346–360.

Balazadeh, S., Parlitz, S., Mueller-Roeber, B., and Meyer, R.C. (2008a). Natural developmental variations in leaf and plant senescence in *Arabidopsis thaliana*. Plant Biol. (Stuttg.) **10** (suppl. 1): 136–147.

Balazadeh, S., Riaño-Pachón, D.M., and Mueller-Roeber, B. (2008b). Transcription factors regulating leaf senescence in *Arabidopsis thaliana*. Plant Biol. (Stuttg.) **10** (suppl. 1): 63–75.

Balazadeh, S., Siddiqui, H., Allu, A.D., Matallana-Ramirez, L.P., Caldana, C., Mehrnia, M., Zanor, M.-I., Köhler, B., and Mueller-Roeber, B. (2010a). A gene regulatory network controlled by the NAC transcription factor ANAC092/AtNAC2/ORE1 during salt-promoted senescence. Plant J. **62:** 250–264.

Balazadeh, S., Wu, A.H., and Mueller-Roeber, B. (2010b). Salt-triggered expression of the ANAC092-dependent senescence regulon in *Arabidopsis thaliana*. Plant Signal. Behav. **5:** 1–3.

Barth, C., Moeder, W., Klessig, D.F., and Conklin, P.L. (2004). The timing of senescence and response to pathogens is altered in the ascorbate-deficient *Arabidopsis* mutant vitamin c-1. Plant Physiol. **134:** 1784–1792.

Bhatnagar-Mathur, P., Vadez, V., and Sharma, K.K. (2008). Transgenic approaches for abiotic stress tolerance in plants: Retrospect and prospects. Plant Cell Rep. **27:** 411–424.

Bohnert, H.J., Nelson, D.E., and Jensen, R.G. (1995). Adaption to environmental stresses. Plant Cell **7:** 1099–1111.

Bradford, M.M. (1976). A rapid and sensitive method for the quantitation of microgram quantities of protein utilizing the principle of protein-dye binding. Anal. Biochem. **72:** 248–254.

Breeze, E., et al. (2011). High-resolution temporal profiling of transcripts during *Arabidopsis* leaf senescence reveals a distinct chronology of processes and regulation. Plant Cell **23:** 873–894.

Buchanan-Wollaston, V., Page, T., Harrison, E., Breeze, E., Lim, P.O., Nam, H.G., Lin, J.F., Wu, S.H., Swidzinski, J., Ishizaki, K., and Leaver, C.J. (2005). Comparative transcriptome analysis reveals significant differences in gene expression and signalling pathways between developmental and dark/starvation-induced senescence in *Arabidopsis*. Plant J. **42:** 567–585.

Caldana, C., Scheible, W.R., Mueller-Roeber, B., and Ruzicic, S. (2007). A quantitative RT-PCR platform for high-throughput expression profiling of 2500 rice transcription factors. Plant Methods **3:** 7.

Chung, J.S., Zhu, J.K., Bressan, R.A., Hasegawa, P.M., and Shi, H.Z. (2008). Reactive oxygen species mediate Na+-induced SOS1 mRNA stability in *Arabidopsis*. Plant J. **53:** 554–565.

Davletova, S., Rizhsky, L., Liang, H., Shengqiang, Z., Oliver, D.J., Coutu, J., Shulaev, V., Schlauch, K., and Mittler, R. (2005a). Cytosolic ascorbate peroxidase 1 is a central component of the reactive oxygen gene network of *Arabidopsis*. Plant Cell **17:** 268–281.

Davletova, S., Schlauch, K., Coutu, J., and Mittler, R. (2005b). The zinc-finger protein Zat12 plays a central role in reactive oxygen and abiotic stress signaling in Arabidopsis. Plant Physiol. **139:** 847–856.

Dhindsa, R.S., Dhindsa, P.P., and Thorpe, T.A. (1981). Leaf senescence: Correlated with increased levels membrane permeability and lipid peroxidation and decreased levels of SOD and CAT. J. Exp. Bot. **32:** 93–101.

Diaz, C., Saliba-Colombani, V., Loudet, O., Belluomo, P., Moreau, L., Daniel-Vedele, F., Morot-Gaudry, J.F., and Masclaux-Daubresse, C. (2006). Leaf yellowing and anthocyanin accumulation are two genetically independent strategies in response to nitrogen limitation in *Arabidopsis thaliana*. Plant Cell Physiol. **47:** 74–83.

Djilianov, D., Georgieva, T., Moyankova, D., Atanassov, A., Shinozaki, K., Smeeken, S.C.M., Verma, D.P.S., and Murata, N. (2005). Improved abiotic stress tolerance in plants by accumulation of osmoprotectants - Gene transfer approach. Biotechnol. Biotechnol. Equip. **19** (Special Issue): 63–71.

Dwidedi, S., Kar, M., and Mishra, D. (1979). Biochemical changes in excised leaves of *Oryza sativa* subjected to water stress. Physiol. Plant. **45:** 35–40.

Finkel, T., and Holbrook, N.-J. (2000). Oxidants, oxidative stress and the biology of ageing. Nature **408:** 239–247.

Fryer, M.J., Oxborough, K., Mullineaux, P.M., and Baker, N.R. (2002). Imaging of photo-oxidative stress responses in leaves. J. Exp. Bot. **53:** 1249–1254.

Gadjev, I., Vanderauwera, S., Gechev, T.S., Laloi, C., Minkov, I.N., Shulaev, V., Apel, K., Inzé, D., Mittler, R., and Van Breusegem, F. (2006). Transcriptomic footprints disclose specificity of reactive oxygen species signaling in Arabidopsis. Plant Physiol. **141:** 436–445.

Gan, S., and Amasino, R.M. (1995). Inhibition of leaf senescence by autoregulated production of cytokinin. Science **270:** 1986–1988.

Gechev, T.S., Gadjev, I.Z., and Hille, J. (2004). An extensive microarray analysis of AAL-toxin-induced cell death in *Arabidopsis thaliana* brings new insights into the complexity of programmed cell death in plants. Cell. Mol. Life Sci. **61:** 1185–1197.

Gechev, T.S., and Hille, J. (2005). Hydrogen peroxide as a signal controlling plant programmed cell death. J. Cell Biol. **168:** 17–20.

Gechev, T.S., Minkov, I.N., and Hille, J. (2005). Hydrogen peroxide-induced cell death in *Arabidopsis*: Transcriptional and mutant analysis reveals a role of an oxoglutarate-dependent dioxygenase gene in the cell death process. IUBMB Life **57:** 181–188.

Gepstein, S., Sabehi, G., Carp, M.J., Hajouj, T., Nesher, M.F., Yariv, I., Dor, C., and Bassani, M. (2003). Large-scale identification of leaf senescence-associated genes. Plant J. **36:** 629–642.

Gill, S.S., and Tuteja, N. (2010). Polyamines and abiotic stress tolerance in plants. Plant Signal. Behav. **5:** 26–33.

Gregersen, P.L., and Holm, P.B. (2007). Transcriptome analysis of senescence in the flag leaf of wheat (*Triticum aestivum* L.). Plant Biotechnol. J. **5:** 192–206.

Guo, Y., Cai, Z., and Gan, S. (2004). Transcriptome of *Arabidopsis* leaf senescence. Plant Cell Environ. **27:** 521–549.

Guo, Y., and Gan, S. (2006). AtNAP, a NAC family transcription factor, has an important role in leaf senescence. Plant J. **46:** 601–612.

He, Y., and Gan, S. (2002). A gene encoding an acyl hydrolase is involved in leaf senescence in *Arabidopsis*. Plant Cell **14:** 805–815.

Hinderhofer, K., and Zentgraf, U. (2001). Identification of a transcription factor specifically expressed at the onset of leaf senescence. Planta **213:** 469–473.

Hirai, M.Y., et al. (2007). Omics-based identification of Arabidopsis Myb transcription factors regulating aliphatic glucosinolate biosynthesis. Proc. Natl. Acad. Sci. USA **104:** 6478–6483.

Hoch, W.A., Singsaas, E.L., and McCown, B.H. (2003). Resorption protection. Anthocyanins facilitate nutrient recovery in autumn by shielding leaves from potentially damaging light levels. Plant Physiol. **133:** 1296–1305.

Hu, R., Qi, G., Kong, Y., Kong, D., Gao, Q., and Zhou, G. (2010). Comprehensive analysis of NAC domain transcription factor gene family in *Populus trichocarpa*. BMC Plant Biol. **10:** 145.

Jefferson, R.A., Kavanagh, T.A., and Bevan, M.W. (1987). GUS fusions: β-Glucuronidase as a sensitive and versatile gene fusion marker in higher plants. EMBO J. **6:** 3901–3907.

Jing, H.-C., Hille, J., and Dijkwel, P.P. (2003). Ageing in plants: Conserved strategies and novel pathways. Plant Biol. **5:** 455–464.

Kant, P., Gordon, M., Kant, S., Zolla, G., Davydov, O., Heimer, Y.M., Chalifa-Caspi, V., Shaked, R., and Barak, S. (2008). Functional-genomics-based identification of genes that regulate *Arabidopsis* responses to multiple abiotic stresses. Plant Cell Environ. **31:** 697–714.

Kasuga, M., Liu, Q., Miura, S., Yamaguchi-Shinozaki, K., and

Shinozaki, K. (1999). Improving plant drought, salt, and freezing tolerance by gene transfer of a single stress-inducible transcription factor. Nat. Biotechnol. **17:** 287–291.

Kaufmann, K., Muiño, J.M., Østerås, M., Farinelli, L., Krajewski, P., and Angenent, G.C. (2010). Chromatin immunoprecipitation (ChIP) of plant transcription factors followed by sequencing (ChIP-SEQ) or hybridization to whole genome arrays (ChIP-CHIP). Nat. Protoc. **5:** 457–472.

Kim, J.H., Woo, H.R., Kim, J., Lim, P.O., Lee, I.C., Choi, S.H., Hwang, D., and Nam, H.G. (2009). Trifurcate feed-forward regulation of age-dependent cell death involving *miR164* in *Arabidopsis*. Science **323:** 1053–1057.

Kopka, J., et al. (2005). GMD@CSB.DB: The Golm Metabolome Database. Bioinformatics **21:** 1635–1638.

Kurepa, J., Smalle, J., Van Montagu, M., and Inzé, D. (1998). Oxidative stress tolerance and longevity in *Arabidopsis*: The late-flowering mutant *gigantea* is tolerant to paraquat. Plant J. **14:** 759–764.

Levey, S., and Wingler, A. (2005). Natural variation in the regulation of leaf senescence and relation to other traits in *Arabidopsis*. Plant Cell Environ. **28:** 223–231.

Licausi, F., Weits, D.A., Pant, B.D., Scheible, W.R., Geigenberger, P., and van Dongen, J.T. (2011). Hypoxia responsive gene expression is mediated by various subsets of transcription factors and miRNAs that are determined by the actual oxygen availability. New Phytol. **190:** 442–456.

Lim, P.O., Kim, H.J., and Nam, H.G. (2007). Leaf senescence. Annu. Rev. Plant Biol. **58:** 115–136.

Lin, J.F., and Wu, S.H. (2004). Molecular events in senescing *Arabidopsis* leaves. Plant J. **39:** 612–628.

Lisec, J., Schauer, N., Kopka, J., Willmitzer, L., and Fernie, A.R. (2006). Gas chromatography mass spectrometry-based metabolite profiling in plants. Nat. Protoc. **1:** 387–396.

Liu, Q., Kasuga, M., Sakuma, Y., Abe, H., Miura, S., Yamaguchi-Shinozaki, K., and Shinozaki, K. (1998). Two transcription factors, DREB1 and DREB2, with an EREBP/AP2 DNA binding domain separate two cellular signal transduction pathways in drought- and low-temperature-responsive gene expression, respectively, in *Arabidopsis*. Plant Cell **10:** 1391–1406.

Miao, Y., Laun, T., Zimmermann, P., and Zentgraf, U. (2004). Targets of the WRKY53 transcription factor and its role during leaf senescence in *Arabidopsis*. Plant Mol. Biol. **55:** 853–867.

Muller, F.L., Lustgarten, M.S., Jang, Y., Richardson, A., and Van Remmen, H. (2007). Trends in oxidative aging theories. Free Radic. Biol. Med. **43:** 477–503.

Müller, J., Boller, T., and Wiemken, A. (1995). Trehalose and trehalase in plants: recent developments. Plant Sci. **112:** 1–9.

Nakabayashi, R., Kusano, M., Kobayashi, M., Tohge, T., Yonekura-Sakakibara, K., Kogure, N., Yamazaki, M., Kitajima, M., Saito, K., and Takayama, H. (2009). Metabolomics-oriented isolation and structure elucidation of 37 compounds including two anthocyanins from *Arabidopsis thaliana*. Phytochemistry **70:** 1017–1029.

Navabpour, S., Morris, K., Allen, R., Harrison, E., A-H-Mackerness, S., and Buchanan-Wollaston, V. (2003). Expression of senescence-enhanced genes in response to oxidative stress. J. Exp. Bot. **54:** 2285–2292.

Nishizawa, A., Yabuta, Y., Yoshida, E., Maruta, T., Yoshimura, K., and Shigeoka, S. (2006). *Arabidopsis* heat shock transcription factor A2 as a key regulator in response to several types of environmental stress. Plant J. **48:** 535–547.

Nishizawa-Yokoi, A., Nosaka, R., Hayashi, H., Tainaka, H., Maruta, T., Tamoi, M., Ikeda, M., Ohme-Takagi, M., Yoshimura, K., Yabuta, Y., and Shigeoka, S. (2011). HsfA1d and HsfA1e involved in the transcriptional regulation of *HsfA2* function as key regulators for the Hsf signaling network in response to environmental stress. Plant Cell Physiol. **52:** 933–945.

Noh, Y.-S., and Amasino, R.M. (1999). Identification of a promoter region responsible for the senescence-specific expression of *SAG12*. Plant Mol. Biol. **41:** 181–194.

Noodén, L.D., Guiamét, J.J., and John, I. (1997). Senescence mechanisms. Physiol. Plant. **101:** 746–753.

Ooka, H., et al. (2003). Comprehensive analysis of NAC family genes in *Oryza sativa* and *Arabidopsis thaliana*. DNA Res. **10:** 239–247.

Parlitz, S., Kunze, R., Mueller-Roeber, B., and Balazadeh, S. (2011). Regulation of photosynthesis and transcription factor expression by leaf shading and re-illumination in *Arabidopsis thaliana* leaves. J. Plant Physiol. **168:** 1311–1319.

Plesch, G., Ehrhardt, T., and Mueller-Roeber, B. (2001). Involvement of TAAAG elements suggests a role for Dof transcription factors in guard cell-specific gene expression. Plant J. **28:** 455–464.

Qin, F., et al. (2008). *Arabidopsis* DREB2A-interacting proteins function as RING E3 ligases and negatively regulate plant drought stress-responsive gene expression. Plant Cell **20:** 1693–1707.

Rentel, M.C., Lecourieux, D., Ouaked, F., Usher, S.L., Petersen, L., Okamoto, H., Knight, H., Peck, S.C., Grierson, C.S., Hirt, H., and Knight, M.R. (2004). OXI1 kinase is necessary for oxidative burst-mediated signalling in *Arabidopsis*. Nature **427:** 858–861.

Reth, M. (2002). Hydrogen peroxide as second messenger in lymphocyte activation. Nat. Immunol. **3:** 1129–1134.

Roessner, U., Luedemann, A., Brust, D., Fiehn, O., Linke, T., Willmitzer, L., and Fernie, A.R. (2001). Metabolic profiling allows comprehensive phenotyping of genetically or environmentally modified plant systems. Plant Cell **13:** 11–29.

Sakuma, Y., Maruyama, K., Osakabe, Y., Qin, F., Seki, M., Shinozaki, K., and Yamaguchi-Shinozaki, K. (2006a). Functional analysis of an *Arabidopsis* transcription factor, DREB2A, involved in drought-responsive gene expression. Plant Cell **18:** 1292–1309.

Sakuma, Y., Maruyama, K., Qin, F., Osakabe, Y., Shinozaki, K., and Yamaguchi-Shinozaki, K. (2006b). Dual function of an *Arabidopsis* transcription factor DREB2A in water-stress-responsive and heat-stress-responsive gene expression. Proc. Natl. Acad. Sci. USA **103:** 18822–18827.

Sambrook, J., Fritsche, E.F., and Maniatis, T. (2001) Molecular Cloning: A Laboratory Manual, 3rd ed. (Cold Spring Harbor, NY: Cold Spring Harbor Laboratory Press).

Schauer, N., Steinhauser, D., Strelkov, S., Schomburg, D., Allison, G., Moritz, T., Lundgren, K., Roessner-Tunali, U., Forbes, M.G., Willmitzer, L., Fernie, A.R., and Kopka, J. (2005). GC-MS libraries for the rapid identification of metabolites in complex biological samples. FEBS Lett. **579:** 1332–1337.

Schramm, F., Ganguli, A., Kiehlmann, E., Englich, G., Walch, D., and von Koskull-Döring, P. (2006). The heat stress transcription factor HsfA2 serves as a regulatory amplifier of a subset of genes in the heat stress response in *Arabidopsis*. Plant Mol. Biol. **60:** 759–772.

Schramm, F., Larkindale, J., Kiehlmann, E., Ganguli, A., Englich, G., Vierling, E., and von Koskull-Döring, P. (2008). A cascade of transcription factor DREB2A and heat stress transcription factor HsfA3 regulates the heat stress response of *Arabidopsis*. Plant J. **53:** 264–274.

Sharabi-Schwager, M., Lers, A., Samach, A., Guy, C.L., and Porat, R. (2010). Overexpression of the CBF2 transcriptional activator in *Arabidopsis* delays leaf senescence and extends plant longevity. J. Exp. Bot. **61:** 261–273.

Sheen, J. (2002). A transient expression assay using *Arabidopsis* mesophyll protoplasts. http://genetics.mgh.harvard.edu/sheenweb/.

Shigeoka, S., Ishikawa, T., Tamoi, M., Miyagawa, Y., Takeda, T.,

Yabuta, Y., and Yoshimura, K. (2002). Regulation and function of ascorbate peroxidase isoenzymes. J. Exp. Bot. **53:** 1305–1319.

Skirycz, A., Reichelt, M., Burow, M., Birkemeyer, C., Rolcik, J., Kopka, J., Zanor, M.I., Gershenzon, J., Strnad, M., Szopa, J., Mueller-Roeber, B., and Witt, I. (2006). DOF transcription factor AtDof1.1 (OBP2) is part of a regulatory network controlling glucosinolate biosynthesis in *Arabidopsis*. Plant J. **47:** 10–24.

Smart, C.M., Hosken, S.E., Thomas, H., Greaves, J.A., Blair, B.G., and Schuch, W. (1995). The timing of maize leaf senescence and characterization of senescence-related cDNAs. Physiol. Plant. **93:** 673–682.

Suzuki, N., Sejima, H., Tam, R., Schlauch, K., and Mittler, R. (2011). Identification of the MBF1 heat-response regulon of *Arabidopsis thaliana*. Plant J. **66:** 844–851.

Swindell, W.R. (2006). The association among gene expression responses to nine abiotic stress treatments in *Arabidopsis thaliana*. Genetics **174:** 1811–1824.

Tohge, T., and Fernie, A.R. (2009). Web-based resources for mass-spectrometry-based metabolomics: A user's guide. Phytochemistry **70:** 450–456.

Tohge, T., and Fernie, A.R. (2010). Combining genetic diversity, informatics and metabolomics to facilitate annotation of plant gene function. Nat. Protoc. **5:** 1210–1227.

Tohge, T., et al. (2005). Functional genomics by integrated analysis of metabolome and transcriptome of *Arabidopsis* plants over-expressing an MYB transcription factor. Plant J. **42:** 218–235.

Tohge, T., Yonekura-Sakakibara, K., Niida, R., Watanabe-Takahashi, A., and Saito, K. (2007). Phytochemical genomics in *Arabidopsis thaliana*: A case study for functional identification of flavonoid biosynthsis genes. Pure Appl. Chem. **79:** 811–823.

Vanderauwera, S., Zimmermann, P., Rombauts, S., Vandenabeele, S., Langebartels, C., Gruissem, W., Inzé, D., and Van Breusegem, F. (2005). Genome-wide analysis of hydrogen peroxide-regulated gene expression in *Arabidopsis* reveals a high light-induced transcriptional cluster involved in anthocyanin biosynthesis. Plant Physiol. **139:** 806–821.

van der Graaff, E., Schwacke, R., Schneider, A., Desimone, M., Flügge, U.I., and Kunze, R. (2006). Transcription analysis of *Arabidopsis* membrane transporters and hormone pathways during developmental and induced leaf senescence. Plant Physiol. **141:** 776–792.

van Doorn, W.G., and Woltering, E.J. (2008). Physiology and molecular biology of petal senescence. J. Exp. Bot. **59:** 453–480.

Verbruggen, N., and Hermans, C. (2008). Proline accumulation in plants: A review. Amino Acids **35:** 753–759.

Woo, H.R., Kim, J.H., Nam, H.G., and Lim, P.O. (2004). The delayed leaf senescence mutants of *Arabidopsis*, *ore1*, *ore3*, and *ore9*, are tolerant to oxidative stress. Plant Cell Physiol. **45:** 923–932.

Xue, G.P. (2002). Characterisation of the DNA-binding profile of barley HvCBF1 using an enzymatic method for rapid, quantitative and high-throughput analysis of the DNA-binding activity. Nucleic Acids Res. **30:** e77.

Xue, G.P. (2005). A CELD-fusion method for rapid determination of the DNA-binding sequence specificity of novel plant DNA-binding proteins. Plant J. **41:** 638–649.

Yamaguchi, M., Ohtani, M., Mitsuda, N., Kubo, M., Ohme-Takagi, M., Fukuda, H., and Demura, T. (2010). VND-INTERACTING2, a NAC domain transcription factor, negatively regulates xylem vessel formation in *Arabidopsis*. Plant Cell **22:** 1249–1263.

Yang, S.D., Seo, P.J., Yoon, H.K., and Park, C.M. (2011). The arabidopsis NAC transcription factor VNI2 integrates abscisic acid signals into leaf senescence via the *COR/RD* genes. Plant Cell **23:** 2155–2168.

Ye, Z., Rodriguez, R., Tran, A., Hoang, H., de los Santos, D., Brown, S., and Vellanoweth, R.L. (2000). The developmental transition to flowering represses ascorbate peroxidase activity and induces enzymatic lipid peroxidation in leaf tissue in *Arabidopsis thaliana*. Plant Sci. **158:** 115–127.

Yonekura-Sakakibara, K., Tohge, T., Matsuda, F., Nakabayashi, R., Takayama, H., Niida, R., Watanabe-Takahashi, A., Inoue, E., and Saito, K. (2008). Comprehensive flavonol profiling and transcriptome coexpression analysis leading to decoding gene-metabolite correlations in *Arabidopsis*. Plant Cell **20:** 2160–2176.

Yoo, S.D., Cho, Y.H., and Sheen, J. (2007). *Arabidopsis* mesophyll protoplasts: A versatile cell system for transient gene expression analysis. Nat. Protoc. **2:** 1565–1572.

Yoshiba, Y., Kiyosue, T., Nakashima, K., Yamaguchi-Shinozaki, K., and Shinozaki, K. (1997). Regulation of levels of proline as an osmolyte in plants under water stress. Plant Cell Physiol. **38:** 1095–1102.

Yoshida, T., Sakuma, Y., Todaka, D., Maruyama, K., Qin, F., Mizoi, J., Kidokoro, S., Fujita, Y., Shinozaki, K., and Yamaguchi-Shinozaki, K. (2008). Functional analysis of an *Arabidopsis* heat-shock transcription factor HsfA3 in the transcriptional cascade downstream of the DREB2A stress-regulatory system. Biochem. Biophys. Res. Commun. **368:** 515–521.

Zimmermann, P., Heinlein, C., Orendi, G., and Zentgraf, U. (2006). Senescence-specific regulation of catalases in *Arabidopsis thaliana* (L.) Heynh. Plant Cell Environ. **29:** 1049–1060.

Zuo, J., Niu, Q.-W., and Chua, N.-H. (2000). Technical advance: An estrogen receptor-based transactivator XVE mediates highly inducible gene expression in transgenic plants. Plant J. **24:** 265–273.

JUNGBRUNNEN1, a Reactive Oxygen Species–Responsive NAC Transcription Factor, Regulates Longevity in *Arabidopsis*

Anhui Wu, Annapurna Devi Allu, Prashanth Garapati, Hamad Siddiqui, Hakan Dortay, Maria-Inés Zanor, Maria Amparo Asensi-Fabado, Sergi Munné-Bosch, Carla Antonio, Takayuki Tohge, Alisdair R. Fernie, Kerstin Kaufmann, Gang-Ping Xue, Bernd Mueller-Roeber and Salma Balazadeh

Plant Cell 2012;24;482-506; originally published online February 17, 2012;
DOI 10.1105/tpc.111.090894

This information is current as of January 10, 2013

Supplemental Data	**http://www.plantcell.org/content/suppl/2012/02/13/tpc.111.090894.DC1.html**
References	This article cites 100 articles, 37 of which can be accessed free at: http://www.plantcell.org/content/24/2/482.full.html#ref-list-1
Permissions	https://www.copyright.com/ccc/openurl.do?sid=pd_hw1532298X&issn=1532298X&WT.mc_id=pd_hw1532298X
eTOCs	Sign up for eTOCs at: http://www.plantcell.org/cgi/alerts/ctmain
CiteTrack Alerts	Sign up for CiteTrack Alerts at: http://www.plantcell.org/cgi/alerts/ctmain
Subscription Information	Subscription Information for *The Plant Cell* and *Plant Physiology* is available at: http://www.aspb.org/publications/subscriptions.cfm

© American Society of Plant Biologists
ADVANCING THE SCIENCE OF PLANT BIOLOGY